The SETUPS object of the CP-PAW code

Peter E. Blöchl

Institute of Theoretical Physics; Clausthal University of Technology;
D-38678 Clausthal Zellerfeld; Germany;
http://www.pt.tu-clausthal.de/atp/

Contents

0.1 Important notes

- The atomic calculation has been performed in a box equal to rout=r(nr-3). The size of the box for the atom is thus defined by the grid. This is ok.

  The radius rbox selects the partial waves in the traditional construction: Those partial waves are selected that have the same logarithmic derivative at the radius rbox. In the new construction, which is based on a Taylor expansion, on the other hand the radius rbox has no function.

  The matrix elements of the potential energy for dh have been calculated only up to the rbnd=rbox. which is smaller than rout. This is now changed and produces different results.

- Tsequentialaugment is not relevant for the total energies of a pure dft calculation. The changes for Si2 have been less than μH for individual energies and less for the converged total energy.

Chapter 1

Purpose and theoretical background

The nodeless construction is proposed by Blöchl and Först[1].

1.1 Nodeless constructiuon

1.1.1 Basic definitions

Energy-dependent partial waves

Let us consider a spherical one-particle Hamiltonian $\hat{h}$. We construct energy-dependent partial waves by radially integrating the radial Schrödinger equation

$$(\hat{h} - \epsilon)|\phi_{ref}(\epsilon)\rangle = 0 \tag{1.1}$$

outward with the boundary conditions

$$\lim_{|\vec{r}|\to 0} \frac{\phi_{ref}(\epsilon, \vec{r})}{|\vec{r}|^{\ell} Y_{\ell,m}(\vec{r})} = 1 \tag{1.2}$$

at the origin. That is, the radial parts of all partial wave behave at the origin like r^{ℓ}. We use the subscript ref to distinguish it from the partial waves introduced later, which differ by an energy-dependent scale factor.

The only difference to the common construction is that we do not normalize the partial waves within a sphere, but by the boundary conditions at the origin. That is, we effectively shrink the normalization sphere to zero.

Node-less bound states

We define[1] a sequence of **node-less bound states** $|u_n\rangle$. The node-less bound state are constructed sequentially by

$$(\hat{h} - \epsilon_n)|u_n\rangle = -|u_{n-1}\rangle\,. \tag{1.3}$$

The first wave function, $|u_1\rangle$ is the lowest bound state of the Hamiltonian. The other wave functions are obtained by radially integrating the Schrödinger equation outward, starting with

vanishing value and derivative, so that

$$\lim_{\vec{r}\to 0} \frac{\langle \vec{r}|u_n\rangle}{|\vec{r}|^{\ell+1}} = 0 \qquad \text{for } n > 1 \tag{1.4}$$

The node-less wave functions $|u_n\rangle$ do not have any nodes, but look like Slater orbitals, in the sense that they grow at the origin as a power and that they decay exponentially at large distance. Their behavior at the origin is[1]

$$u_n(\vec{r}) = \left(\frac{2m_e}{\hbar^2}\right)^{n-1} \frac{(2\ell+1)!!}{(2\ell-1+2n)!!(2n-2)!!} |\vec{r}|^{\ell+2(n-1)} Y_{\ell,m}(\vec{r}) \tag{1.5}$$

where $Y_{\ell,m}$ is a real spherical harmonics.

The n lowest node-less wave functions span the same Hilbert space as the n lowest true wave functions. The all-electron wave functions can be recovered from the node-less wave functions via[1]

$$|\phi_{ref,n}\rangle = \sum_{m=1}^{n} |u_m\rangle \prod_{j=1}^{m-1} (\epsilon_j - \epsilon_n) = \left[\sum_{m=1}^{n} |u_m\rangle \prod_{j=m}^{n-1} \frac{1}{(\epsilon_j - \epsilon_n)}\right] \prod_{k=1}^{n-1} (\epsilon_k - \epsilon_n) \tag{1.6}$$

Node-reduced partial waves

Secondly, we define [1] a sequence of energy-dependent **node-reduced partial waves** $|q_n(\epsilon)\rangle$ through

$$(\hat{h} - \epsilon)|q_n(\epsilon)\rangle = -|u_{n-1}\rangle \tag{1.7}$$

with the boundary conditions

$$\lim_{\vec{r}\to 0} \frac{\langle \vec{r}|q_n(\epsilon)\rangle}{\langle \vec{r}|u_n\rangle} = 1 \qquad \text{for } n > 1 \tag{1.8}$$

The node-reduced wave functions have (typically[1]) $n-1$ nodes less than the true wave function. Near the origin, they are very similar to $|u_n\rangle$ over nearly the entire energy range.

The all-electron partial wave $|\phi(\epsilon)\rangle$ can be constructed from the node-reduced partial wave $|q_n(\epsilon)\rangle$ and the lower node-less bound states $|u_m\rangle$ as[1]

$$|\phi_{ref}(\epsilon)\rangle = \left[|q_n(\epsilon)\rangle + \sum_{m=1}^{n-1} |u_m\rangle \prod_{j=m}^{n-1} \frac{1}{\epsilon_j - \epsilon}\right] \prod_{k=1}^{n-1} (\epsilon_k - \epsilon) \tag{1.9}$$

In practice we focus on the particular node-reduced wave functions, for which the nodes of all core states are eliminated, that is for which $n = n_c + 1$ is the quantum number of the lowest valence (non-core) state.

[1] As shown in [1], the nodal theorem fails at high energies, so that the statement is correct for practical purposes, but incorrect in a strict sense.

In order to avoid the scale factor $\prod_{k=1}^{n-1}(\epsilon_k - \epsilon)$, we introduce a new all-electron partial wave $|\phi_n(\epsilon)\rangle$

$$\begin{aligned} |\phi_n(\epsilon)\rangle &\stackrel{\text{def}}{=} |\phi_{ref}(\epsilon)\rangle \frac{1}{\prod_{k=1}^{n-1}(\epsilon_k - \epsilon)} \\ &= |q_n(\epsilon)\rangle + \sum_{m=1}^{n-1} |u_m\rangle \prod_{j=m}^{n-1} \frac{1}{\epsilon_j - \epsilon} \end{aligned} \tag{1.10}$$

Series expansion of the node-reduced partial wave

Let us now define [1] a new sequence of nodeless functions for given set of energies $\{\epsilon_{n+j}; j \geq 1\}$ via

$$(\hat{h} - \epsilon)|\bar{q}_n^{(j)}(\epsilon)\rangle = -|\bar{q}_n^{(j-1)}(\epsilon_{n+j-1})\rangle \tag{1.11}$$

$$(\hat{h} - \epsilon)|\bar{q}_n^{(0)}(\epsilon)\rangle = -|u_{n-1}\rangle \tag{1.12}$$

where $|\bar{q}_n^{(0)}(\epsilon)\rangle = |\bar{q}_n(\epsilon)\rangle$ defined in Eq. 1.7. Eq. 1.12 and Eq. 1.11 have great similarity with those of the nodeless equations Eq. 1.3.

The sequence defined by Eq. 1.11 and Eq. 1.12 can be constructed by the recursive equation

$$\begin{aligned} |\bar{q}_n^{(j+1)}(\epsilon)\rangle &= \frac{-1}{\epsilon - \epsilon_{n+j}} \Big(|\bar{q}_n^{(j)}(\epsilon)\rangle - |\bar{q}_n^{(j)}(\epsilon_{n+j})\rangle \Big) \qquad \text{for } \epsilon \neq \epsilon_{n+j} \\ |\bar{q}_n^{(j+1)}(\epsilon_{n+j})\rangle &= -\partial_\epsilon|_{\epsilon_{n+j}} |\bar{q}_n^{(j)}(\epsilon)\rangle \end{aligned} \tag{1.13}$$

Eq. 1.13 is shown recursively: We assume that Eq. 1.11 holds for j and show that Eq. 1.13 obeys Eq. 1.11 for $j+1$.

$$\begin{aligned} (\hat{h} - \epsilon)|\bar{q}_n^{(j+1)}(\epsilon)\rangle &\stackrel{\text{Eq. 1.13}}{=} \frac{-1}{\epsilon - \epsilon_{n+j}} \Big((\hat{h} - \epsilon)|\bar{q}_n^{(j)}(\epsilon)\rangle - (\hat{h} - \epsilon_{n+j})|\bar{q}_n^{(j)}(\epsilon_{n+j})\rangle + (\epsilon - \epsilon_{n+j})|\bar{q}_n^{(j)}(\epsilon_{n+j})\rangle \Big) \\ &\stackrel{\text{Eq. 1.11}}{=} \frac{-1}{\epsilon - \epsilon_{n+j}} \Big(\underbrace{-|\bar{q}_n^{(j-1)}(\epsilon_{n+j-1})\rangle + |\bar{q}_n^{(j-1)}(\epsilon_{n+j-1})\rangle}_{=0} + (\epsilon - \epsilon_{n+j})|\bar{q}_n^{(j)}(\epsilon_{n+j})\rangle \Big) \\ &= -|\bar{q}_n^{(j)}(\epsilon_{n+j})\rangle \end{aligned} \tag{1.14}$$

which is Eq. 1.11 for the next higher value of j. This completes the proof that $|q_n^{(j)}(\epsilon)\rangle$ defined in Eq. 1.11 obeys the recursion Eq. 1.13.

From the series defined by Eq. 1.11 and Eq. 1.12, we can again recover the node-reduced partial wave as

$$\begin{aligned} |q_n(\epsilon)\rangle &= |\bar{q}_n^{(0)}(\epsilon)\rangle \\ &\stackrel{\text{Eq. 1.13}}{=} |\bar{q}_n^{(0)}(\epsilon_n)\rangle + |\bar{q}_n^{(1)}(\epsilon)\rangle(\epsilon_n - \epsilon) \\ &\stackrel{\text{Eq. 1.13}}{=} |\bar{q}_n^{(0)}(\epsilon_n)\rangle + |\bar{q}_n^{(1)}(\epsilon_{n+1})\rangle(\epsilon_n - \epsilon) + |\bar{q}_n^{(2)}(\epsilon)\rangle(\epsilon_{n+1} - \epsilon)(\epsilon_n - \epsilon) \\ &= \left(\sum_{k=0}^{j-1} |\bar{q}_n^{(k)}(\epsilon_{n+k})\rangle \prod_{m=0}^{k-1} (\epsilon_{n+m} - \epsilon) \right) + |\bar{q}_n^{(j)}(\epsilon)\rangle \prod_{m=0}^{j-1} (\epsilon_{n+m} - \epsilon) \end{aligned} \tag{1.15}$$

In this derivation, no assumptions have been made regarding the energies ϵ_{n+j}. The value of j is arbitrary.

In the special case that all energies ϵ_{n+k} are chosen to be identical, the series expansion Eq. 1.13 produces the Taylor-expansion coefficients

$$|\bar{q}_n^{(j)}(\epsilon)\rangle = \frac{(-1)^j}{j!}\partial_\epsilon^j |q_n(\epsilon)\rangle \tag{1.16}$$

Using all energies equal, Eq. 1.15 results in the Taylor series with coefficients from Eq. 1.16.

Using instead bound-state energies in sequence, Eq. 1.11 and Eq. 1.12 results in a nodeless construction.

This flexibility can be exploited to set up an expansion with bound states and with scattering states. This is important if we wish to describe semi-core states, valence states and scattering states on the same footing.

From Eq. 1.10 and Eq. 1.15, we obtain the expression for the full energy-dependent wave function, which holds for arbitrary values of j.

$$|\phi_n(\epsilon)\rangle = \underbrace{|\bar{q}_n^{(j)}(\epsilon)\rangle \left(\prod_{m=0}^{j-1}(\epsilon_{n+m}-\epsilon)\right) + \sum_{k=0}^{j-1}|\bar{q}_n^{(k)}(\epsilon_{n+k})\rangle \left(\prod_{m=0}^{k-1}(\epsilon_{n+m}-\epsilon)\right)}_{|q_n(\epsilon)\rangle}$$
$$+ \underbrace{\left(\sum_{m=1}^{n-1}|u_m\rangle \prod_{j=m}^{n-1}\frac{1}{\epsilon_j-\epsilon}\right)}_{\text{core contribution}} \tag{1.17}$$

Interesting is that the energy-dependent function $|\bar{q}^{(j)}(\epsilon)\rangle$ does not contribute to the full wave function at the energies ϵ_j of the core states and at the energies ϵ_{n+m} with $m < j$.

1.1.2 Augmentation from node-reduced wave functions

Pseudization

The node-reduced wave function $|q_n(\epsilon)\rangle$ have a similar shape in the central region over the entire energy region. This suggests to change them by the same, energy-independent function $|k\rangle$, because this is likely not to introduce extra nodes and to produce wave functions that are equally suited for a plane wave expansion.

Thus we obtain a definition of our pseudo partial waves over the entire energy region

$$|\tilde{\phi}_n(\epsilon)\rangle = |q_n(\epsilon)\rangle + |k\rangle \tag{1.18}$$

Having a well behaved representation of the pseudo partial waves, we can be quite sure that we do not add ghost states. If each partial wave is pseudized individually, one easily obtains a polynomial representation of the energy-dependent partial wave that contains divergences. The construction of $|k\rangle$ is described in section 1.1.3.

Truncation of the series expansion

Now we introduce a parameter N_j which replaces the arbitrary j in Eq. 1.17

$$|\phi_n(\epsilon)\rangle \overset{\text{Eq. } 1.17}{=} \underbrace{|\bar{q}_n^{(N_j)}(\epsilon)\rangle \left(\prod_{m=0}^{N_j-1}(\epsilon_{n+m}-\epsilon)\right) + \sum_{k=0}^{N_j-1}|\bar{q}_n^{(k)}(\epsilon_{n+k})\rangle \left(\prod_{m=0}^{k-1}(\epsilon_{n+m}-\epsilon)\right)}_{|q_n(\epsilon)\rangle}$$
$$+ \underbrace{\left(\sum_{m=1}^{n-1}|u_m\rangle \prod_{j=m}^{n-1}\frac{1}{\epsilon_j-\epsilon}\right)}_{\text{core contribution}} \tag{1.19}$$

$$|\tilde{\phi}_n(\epsilon)\rangle \overset{\text{Eq. } 1.17}{=} \underbrace{|\bar{q}_n^{(N_j)}(\epsilon)\rangle \left(\prod_{m=0}^{N_j-1}(\epsilon_{n+m}-\epsilon)\right) + \sum_{k=0}^{N_j-1}|\bar{q}_n^{(k)}(\epsilon_{n+k})\rangle \left(\prod_{m=0}^{k-1}(\epsilon_{n+m}-\epsilon)\right)}_{|q_n(\epsilon)\rangle}$$
$$+|k\rangle \tag{1.20}$$

The contribution of the energy-dependent partial wave $|\bar{q}_n^{(N_j)}(\epsilon)\rangle$ is the same in both expressions. This suggests introduce an approximation which ignores this contribution: we truncate the expansion for the energy-dependent partial wave to N_j terms. n is the band index of the lowest valence (non-core) state.

$$|\phi_n(\epsilon)\rangle \approx \sum_{k=0}^{N_j-1}|\bar{q}_n^{(k)}(\epsilon_{n+k})\rangle \prod_{m=0}^{k-1}(\epsilon_{n+m}-\epsilon) + \underbrace{\sum_{m=1}^{n-1}|u_m\rangle \prod_{j=m}^{n-1}\frac{1}{\epsilon_j-\epsilon}}_{\text{core contribution}}$$
$$|\tilde{\phi}_n(\epsilon)\rangle \approx \sum_{k=0}^{N_j-1}|\bar{q}_n^{(k)}(\epsilon_{n+k})\rangle \prod_{m=0}^{k-1}(\epsilon_{n+m}-\epsilon) + |k\rangle \tag{1.21}$$

This representation of the energy-dependent partial wave is exact for the energies ϵ_{n+j} for $0 \le j \le N_j - 1$. The difference between both expressions is exact over the entire energy range.

A basis set describing the pseudo partial waves is

$$|\tilde{\phi}_n^{(0)}(\epsilon_n)\rangle = |\bar{q}_n^{(0)}(\epsilon_n)\rangle + |k\rangle$$
$$|\tilde{\phi}_n^{(j)}(\epsilon_{n+j})\rangle = |\bar{q}_n^{(j)}(\epsilon_{n+j})\rangle \qquad \text{for } 1 \le j \le N_j - 1 \tag{1.22}$$

(Remember that $|q_n(\epsilon_n)\rangle = |\bar{q}_n^0(\epsilon_n)\rangle$.) Note, that only the first pseudo partial wave differs from its node-reduced partial wave. This is because the difference $|k\rangle$ has been chosen energy independent.

The construction of the all-electron wave functions $|\phi_n^{(j)}(n+j)\rangle$ is non-trivial: We first consider the nodeless equation without distinguishing between valence and core states. We use these factors to subtract the core states. For the contribution of the valence states, we only subtract the core-conrtibution, namely $|\phi_n^{(m)}\rangle - |q_n^{(m)}\rangle$. The resulting equation can be

implemented recursively.

$$|\phi_n^{(j)}(\epsilon_{n+j})\rangle = |q_n^{(j)}(\epsilon_{n+j})\rangle + \sum_{m=1}^{n-1} |u_m\rangle \prod_{k=m}^{n+j-1} \frac{1}{\epsilon_k - \epsilon_{n+j}} + \sum_{m=0}^{j-1} \Big(|\phi_n^{(m)}(\epsilon_{n+m})\rangle - |q_n^{(m)}(\epsilon_{n+m})\rangle \Big) \prod_{k=m}^{n+j-1} \frac{1}{\epsilon_{n+k} - \epsilon_{n+j}} \tag{1.23}$$

This equation ensures that the partial waves $|\phi_n^{(j)}(\epsilon_{n+j})\rangle$ are orthogonal to the core states.

Core orthogonalization

The all-electron partial waves are obtained from the node-reduced partial waves $|q_n^{(j)}(\epsilon_{n+j})\rangle$ by explicit orthogonalization to the nodeless core states. Here we begin to orthogonalize to the highest core state first and then proceed to the lowest core state.

Note that we do not include a pseudo core into the pseudo partial waves even though we currently still define a pseudo core state. The latter shall be used to construct a pseudo core density.

Construction of bare projector functions

The projector functions must obey the biorthogonality condition and the bare projector functions must fulfill the closure relation

$$|\bar{p}^{(j)}\rangle = (\tilde{h} - \epsilon_{n+j})|\tilde{\phi}_n(\epsilon_{n+j})\rangle \qquad \text{for } j = 0, \ldots, N_j \tag{1.24}$$

which implies that the scattering properties shall be exactly obeyed at the chosen energies ϵ_{n+j}.

The pseudo partial waves at the energies are

$$\begin{aligned} |\tilde{\phi}_n(\epsilon_{n+p})\rangle &\overset{\text{Eq. } 1.21}{=} \sum_{k=0}^{N_j-1} |\bar{q}_n^{(k)}(\epsilon_{n+k})\rangle \underbrace{\prod_{m=0}^{k-1} (\epsilon_{n+m} - \epsilon_{n+p})}_{=0 \text{ for } k \geq p+1} + |k\rangle \\ &= \sum_{k=0}^{p} |\bar{q}_n^{(k)}(\epsilon_{n+k})\rangle \prod_{m=0}^{k-1} (\epsilon_{n+m} - \epsilon_{n+p}) + |k\rangle \\ &\overset{\text{Eq. } 1.22}{=} \sum_{k=0}^{p} |\tilde{\phi}^{(k)}\rangle \prod_{m=0}^{k-1} (\epsilon_{n+m} - \epsilon_{n+p}) \end{aligned} \tag{1.25}$$

(the terms that drop out in the second line vanish because of the energy factor contains a zero term.) Interestingly, this equation not only holds for the truncated expansion of the partial wave, but also for the full one given in Eq. 1.20.

The expression Eq. 1.25 holds strictly, as long as there are no degenerate values in the sequence ϵ_{n+p}. If two or more ϵ_{n+p} are identical, there is only a single independent partial wave for this set of energies. As a result, the space of bare projector functions derived from these partial waves is too small. For each degenerate set of partial waves we need to introduce first and higher derivatives of the partial waves.

The bare projector functions are obtained as follows

$$
\begin{aligned}
(\hat{\tilde{h}} - \epsilon_{n+p})|\tilde{\phi}_n(\epsilon_{n+p})\rangle &\overset{\text{Eq. } 1.25}{=} \sum_{k=0}^{p}(\hat{\tilde{h}} - \epsilon_{n+p})|\tilde{\phi}_n^{(k)}(\epsilon_{n+k})\rangle \prod_{m=0}^{k-1}(\epsilon_{n+m} - \epsilon_{n+p}) \\
&\overset{\text{Eq. } 1.22}{=} (\hat{\tilde{h}} - \epsilon_n)|\tilde{\phi}_n^{(0)}(\epsilon_n)\rangle + |\tilde{\phi}_n^{(0)}(\epsilon_n)\rangle(\epsilon_n - \epsilon_{n+p}) \\
&\quad + \sum_{k=1}^{p}\Big(\hat{h} - \epsilon_{n+k} + \hat{\tilde{h}} - \hat{h}\Big)|\bar{q}_n^{(k)}(\epsilon_{n+k})\rangle \prod_{m=0}^{k-1}(\epsilon_{n+m} - \epsilon_{n+p}) \\
&\quad + \sum_{k=1}^{p}|\bar{q}_n^{(k)}(\epsilon_{n+k})\rangle(\epsilon_{n+k} - \epsilon_{n+p}) \prod_{m=0}^{k-1}(\epsilon_{n+m} - \epsilon_{n+p}) \\
&\overset{\text{Eq. } 1.11}{=} (\hat{\tilde{h}} - \epsilon_n)|\tilde{\phi}_n^{(0)}(\epsilon_n)\rangle + |\tilde{\phi}_n^{(0)}(\epsilon_n)\rangle(\epsilon_n - \epsilon_{n+p}) \\
&\quad - \underbrace{\sum_{k=1}^{p}|q_n^{(k-1)}(\epsilon_{n+k-1})\rangle \prod_{m=0}^{k-1}(\epsilon_{n+m} - \epsilon_{n+p})}_{\sum_{k=0}^{p-1}|q_n^{(k)}(\epsilon_{n+k})\rangle(\epsilon_{n+k} - \epsilon_{n+p}) \prod_{m=0}^{k-1}(\epsilon_{n+m} - \epsilon_{n+p})} \\
&\quad + \sum_{k=1}^{p-1}|q_n^{(k)}(\epsilon_{n+k})\rangle(\epsilon_{n+k} - \epsilon_{n+p}) \prod_{m=0}^{k-1}(\epsilon_{n+m} - \epsilon_{n+p}) \\
&\quad + \sum_{k=1}^{p}(\hat{\tilde{h}} - \hat{h})|q_n^{(k)}(\epsilon_{n+k})\rangle \prod_{m=0}^{k-1}(\epsilon_{n+m} - \epsilon_{n+p}) \\
&= (\hat{\tilde{h}} - \epsilon_n)|\tilde{\phi}^{(0)}\rangle + |\tilde{\phi}^{(0)}\rangle(\epsilon_n - \epsilon_{n+p}) - |q_n^{(0)}(\epsilon_n)\rangle(\epsilon_n - \epsilon_{n+p}) \\
&\quad + \sum_{k=1}^{p}(\hat{\tilde{h}} - \hat{h})|q_n^{(k)}(\epsilon_{n+k})\rangle \prod_{m=0}^{k-1}(\epsilon_{n+m} - \epsilon_{n+p}) \\
&= (\hat{\tilde{h}} - \epsilon_n)|\tilde{\phi}^{(0)}\rangle + \Big[|\tilde{\phi}^{(0)}\rangle - |q_n^{(0)}(\epsilon_n)\rangle\Big](\epsilon_n - \epsilon_{n+p}) \\
&\quad + \sum_{k=1}^{p}(\hat{\tilde{h}} - \hat{h})|q_n^{(k)}(\epsilon_{n+k})\rangle \prod_{m=0}^{k-1}(\epsilon_{n+m} - \epsilon_{n+p}) \\
&= (\hat{\tilde{h}} - \epsilon_n)|\tilde{\phi}^{(0)}\rangle + \Big(|\tilde{\phi}^{(0)}\rangle - |q_n^{(0)}(\epsilon_n)\rangle + (\hat{\tilde{h}} - \hat{h})|q_n^{(1)}(\epsilon_{n+1})\rangle\Big)(\epsilon_n - \epsilon_{n+p}) \\
&\quad + \sum_{k=2}^{p}(\hat{\tilde{h}} - \hat{h})|q_n^{(k)}(\epsilon_{n+k})\rangle \prod_{m=0}^{k-1}(\epsilon_{n+m} - \epsilon_{n+p}) \\
&= \sum_{j=0}^{p}|\bar{p}^{(j)}\rangle \prod_{k=0}^{j-1}(\epsilon_{n+k} - \epsilon_{n+p}) \qquad (1.26)
\end{aligned}
$$

Thus

$$
\Big(\hat{\tilde{h}} - \epsilon_{n+p}\Big)\underbrace{\sum_{j=0}^{p}|\tilde{\phi}^{(j)}(\epsilon_{n+k})\rangle \prod_{k=0}^{j-1}(\epsilon_{n+k} - \epsilon_{n+p})}_{|\tilde{\phi}_n(\epsilon_{n+p})\rangle} = \underbrace{\sum_{j=0}^{p}|\bar{p}^{(j)}\rangle \prod_{k=0}^{j-1}(\epsilon_{n+k} - \epsilon_{n+p})}_{|\bar{p}(\epsilon_{n+p})\rangle} \qquad (1.27)
$$

The bare projector functions can be spanned by the N_j independent functions

$$\begin{aligned}
|\bar{p}^{(0)}\rangle &= (\hat{\tilde{h}} - \epsilon_n)|\tilde{\phi}^{(0)}\rangle \\
|\bar{p}^{(1)}\rangle &= |\tilde{\phi}^{(0)}\rangle - |q_n^{(0)}(\epsilon_n)\rangle + (\hat{\tilde{h}} - \hat{h})|q_n^{(1)}(\epsilon_{n+1})\rangle \\
|\bar{p}^{(j)}\rangle &= (\hat{\tilde{h}} - \hat{h})|q_n^{(j)}(\epsilon_{n+j})\rangle \qquad \text{for } 2 \le j \le N_j
\end{aligned} \tag{1.28}$$

This selection is independent from the choice of the energies ϵ_{n+p} used to define the sequence of node-reduced wave functions. The energies must, however not be chosen identical, because this would produce trivial results. Rather, the limes where the energies become similar must be taken with great care.

It may be interesting to also evaluate energy-dependent projector functions

$$\begin{aligned}
|\bar{p}(\epsilon)\rangle \quad &\overset{\text{def}}{=} \quad \Big(\hat{\tilde{h}} - \epsilon\Big)|\tilde{\phi}_n(\epsilon)\rangle \\
&\overset{\text{Eq. 1.18}}{=} \Big(\hat{\tilde{h}} - \epsilon\Big)\Big(|q_n(\epsilon)\rangle - |q_n(\epsilon_n)\rangle + |\tilde{\phi}_n(\epsilon_n)\rangle\Big) \\
&\overset{\text{Eq. 1.18}}{=} \underbrace{\Big(\hat{h} - \epsilon\Big)|q_n(\epsilon)\rangle}_{|u_{n-1}\rangle} + \Big(\hat{\tilde{h}} - \hat{h}\Big)|q_n(\epsilon)\rangle \\
&- \quad \underbrace{\Big(\hat{h} - \epsilon_n\Big)|q_n(\epsilon_n)\rangle}_{|u_{n-1}\rangle} + \Big(\hat{h} - \epsilon_n - \hat{\tilde{h}} + \epsilon\Big)|q_n(\epsilon_n)\rangle \\
&+ \quad \underbrace{\Big(\hat{\tilde{h}} - \epsilon_n\Big)|\tilde{\phi}_n(\epsilon_n)\rangle}_{=0} + \Big(\epsilon_n - \epsilon\Big)|\tilde{\phi}_n(\epsilon_n)\rangle \\
&= \quad \Big(\hat{\tilde{h}} - \hat{h}\Big)\underbrace{\Big(|q_n(\epsilon)\rangle - |q_n(\epsilon_n)\rangle\Big)}_{|\bar{q}_n^{(1)}(\epsilon)\rangle(\epsilon_n - \epsilon)} + \Big(\epsilon_n - \epsilon\Big)\Big(|\tilde{\phi}_n(\epsilon_n)\rangle - |q_n(\epsilon_n)\rangle\Big) \\
&= \quad \Big[\Big(\hat{\tilde{h}} - \hat{h}\Big)|\bar{q}_n^{(1)}(\epsilon)\rangle + \underbrace{|\tilde{\phi}_n(\epsilon_n)\rangle - |q_n(\epsilon_n)\rangle}_{|k\rangle}\Big]\Big(\epsilon_n - \epsilon\Big)
\end{aligned} \tag{1.29}$$

Bi-orthogonalization

The bi-orthogonalization shall establish

$$\langle p^{(j)}|\tilde{\phi}^{(j')}\rangle = \delta_{j,j'} \tag{1.30}$$

We do this while maintaining the partial waves, i.e.

$$|p^{(j)}\rangle = \sum_n |p'^{(n)}\rangle\Big(\langle p'^{(j)}|\tilde{\phi}^{(n)}\rangle\Big)_{n,j} \tag{1.31}$$

The biorthogonalization deteriorates quickly, if the number of partial waves is increased.

Question: does the integrand for the overlap between projector function and partial wave fall off sufficiently fast with distance? Note, that the partial waves increase exponentially.

The matrix $\langle p'^{(j)}|\tilde{\phi}^{(n)}\rangle$ becomes singular, because the partial waves do not contribute any more in the region, where the pseudo Hamiltonian differs sufficiently from the all-electron Hamiltonian.

Augmentation contribution to matrix elements

$$\begin{aligned} dO_{\alpha,\beta} &= \langle\phi_\alpha|\phi_\beta\rangle - \langle\tilde{\phi}_\alpha|\tilde{\phi}_\beta\rangle \\ dT_{\alpha,\beta} &= \langle\phi_\alpha|\hat{t}|\phi_\beta\rangle - \langle\tilde{\phi}_\alpha|\hat{t}|\tilde{\phi}_\beta\rangle \end{aligned} \tag{1.32}$$

The calculation of these matrix elements becomes substantially more involved in the relativistic case.

Problem: In order to cancel the tails of the core wave functions, the pseudo partial waves must include a pseudo-core contribution. This, however, is likely to produce ghost states. A remedy could be to change the exponentially increasing behavior of the the node-reduced partial waves artificially such that they do no more grow. In that case, the pseudo-core contribution would not harm.

1.1.3 Pseudo wave functions from node-reduced wave functions

Here, the routine `SETUPS_MAKEPSPHI_FLAT` is described. It is used to construct a pseudo wave function for the lowest node-reduced partial wave.

Starting from a wave function $\phi(\vec{r})$, which shall be pseudized, we invert the Schrödinger equation to determine the potential

$$v - \epsilon_\nu = \begin{cases} -\frac{1}{\phi(\vec{r})}\hat{t}\phi(\vec{r}) & \text{for } r > r_c. \\ A + Br^x & \text{for } r < r_c. \end{cases} \tag{1.33}$$

where r_c is the pseudization radius.

$\hat{t}|\phi\rangle$ is a short-hand notation for the result of the kinetic energy operator acting on the partial wave. In the non-relativistic theory $\hat{t} = \frac{\hat{\vec{p}}^2}{2m_0}$, while the expression is more complex in the relativistic theory.

The coefficients A and B are chosen so that the function is differentiable. The parameter x describes how flat the potential in the core region is and how sharp the upturn is, which is required to ensure differentiability.

With Eq. 1.33, we obtain a potential that is shallow and flat inside the pseudization radius. Outside the pseudization radius it is chosen such that partial wave obeys the non-relativistic Schrödinger equation for this potential.

Note that this potential little to do with the all-electron potential, nor with a pseudo potential. It should be viewed merely as a tool to construct partial waves. If this potential wew a constant, the Schrödinger equation would produce a Bessel functions, and its energy derivatives.

Now, we derive for this potential the radial wave function and its first two energy derivatives

$$\begin{aligned}
\Big[\frac{\vec{p}^2}{2m_0}+v-\epsilon_\nu\Big]|f\rangle &= 0\\
\Big[\frac{\vec{p}^2}{2m_0}+v-\epsilon_\nu\Big]|\dot{f}\rangle &= |f\rangle\\
\Big[\frac{\vec{p}^2}{2m_0}+v-\epsilon_\nu\Big]|\ddot{f}\rangle &= 2|\dot{f}\rangle\\
\Big[\frac{\vec{p}^2}{2m_0}+v-\epsilon_\nu\Big]|\dddot{f}\rangle &= 3|\ddot{f}\rangle
\end{aligned} \tag{1.34}$$

At the same time, we determine

$$\begin{aligned}
\hat{t}|f\rangle &= \frac{\hat{\vec{p}}^2}{2m_e}|f\rangle = (\epsilon-v)|f\rangle\\
\hat{t}|\dot{f}\rangle &= \frac{\hat{\vec{p}}^2}{2m_e}|\dot{f}\rangle = |f\rangle+(\epsilon-v)|\dot{f}\rangle\\
\hat{t}|\ddot{f}\rangle &= \frac{\hat{\vec{p}}^2}{2m_e}|\ddot{f}\rangle = 2|\dot{f}\rangle+(\epsilon-v)|\ddot{f}\rangle\\
\hat{t}|\dddot{f}\rangle &= \frac{\hat{\vec{p}}^2}{2m_e}|\dddot{f}\rangle = 3|\ddot{f}\rangle+(\epsilon-v)|\dddot{f}\rangle
\end{aligned} \tag{1.35}$$

Finally, we match these three functions onto the node-reduced wave function so that

$$|\tilde{\phi}\rangle = |f\rangle c_1+|\dot{f}\rangle c_2+|\ddot{f}\rangle c_3+|\dddot{f}\rangle c_4 \tag{1.36}$$

so that value, derivative and (if requested) the kinetic energy density and its derivative at the cutoff radius agree.

The coefficients are computed as follows:

1. we calculate the value and derivative of $\phi, f, \dot{f}, \ddot{f}, \dddot{f}$ and of their kinetic energies.
2. we add $f, \dot{f}$ to $\ddot{f}, \dddot{f}$ so that their value and derivatives at r_c vanish, and we replace ϕ differentiably by $f, \dot{f}$ inside r_c.
   (a) First we extend ϕ differentiable inside r_c using the first two functions f and $\dot{f}$

$$\phi(r) = f(r)c_1+\dot{f}(r)c_2 \tag{1.37}$$

$$\begin{pmatrix}\phi(r_c)\\ \phi'(r_c)\end{pmatrix} = \begin{pmatrix}f(r_c) & \dot{f}(r_c)\\ f'(r_c) & \dot{f}'(r_c)\end{pmatrix}\begin{pmatrix}c_1\\ c_2\end{pmatrix}$$

$$\begin{pmatrix}c_1\\ c_2\end{pmatrix} = \frac{1}{f(r_c)\dot{f}'(r_c)-f'(r_c)\dot{f}(r_c)}\begin{pmatrix}\dot{f}'(r_c) & -\dot{f}(r_c)\\ -f'(r_c) & f(r_c)\end{pmatrix}\begin{pmatrix}\phi(r_c)\\ \phi'(r_c)\end{pmatrix} \tag{1.38}$$

   (b) now we subtract the $f, \dot{f}$ from the remaining two functions so that the resulting g_3, g_4

go differentiably to zero at r_c.

$$
\begin{aligned}
g_3(r) &:= \ddot{f}(r) - f(r)\ddot{c_1^f} - \dot{f}(r)\ddot{c_2^f} \\
g_4(r) &:= \dddot{f}(r) - f(r)\dddot{c_1^f} - \dot{f}(r)\dddot{c_2^f} \\
\begin{pmatrix} \ddot{c_1^f} \\ \ddot{c_2^f} \end{pmatrix} &= \frac{1}{f(r_c)\dot{f}'(r_c) - f'(r_c)\dot{f}(r_c)} \begin{pmatrix} \dot{f}'(r_c) & -\dot{f}(r_c) \\ -f'(r_c) & f(r_c) \end{pmatrix} \begin{pmatrix} \ddot{f}(r_c) \\ \ddot{f}'(r_c) \end{pmatrix}
\end{aligned} \tag{1.39}
$$

3. values and derivatives of the kinetic energies are adjusted consistently.

4. then we add $\ddot{f}$, $\dddot{f}$ to the new ϕ, so that value and derivative of ϕ. With $t_3(r) = \hat{t}g_3(r)$ and $t_4(r) = \hat{t}g_4(r)$

$$
\begin{aligned}
\phi(r) &\leftarrow \phi(r) - g_3(r)c_3 - g_4(r)c_4 \\
\begin{pmatrix} \hat{t}\phi(r_c) \\ (\hat{t}\phi)'(r_c) \end{pmatrix} &= \begin{pmatrix} t_3(r_c) & t_4(r_c) \\ t_3'(r_c) & t_4'(r_c) \end{pmatrix} \begin{pmatrix} c_3 \\ c_4 \end{pmatrix} \\
\begin{pmatrix} c_3 \\ c_4 \end{pmatrix} &= \frac{1}{t_3(r_c)t_4'(r_c) - t_3'(r_c)t_4(r_c)} \begin{pmatrix} t_4'(r_c) & -t_4(r_c) \\ -t_3'(r_c) & t_3(r_c) \end{pmatrix} \begin{pmatrix} \hat{t}\phi(r_c) \\ (\hat{t}\phi)'(r_c) \end{pmatrix}
\end{aligned} \tag{1.40}
$$

Thus we end up with a pseudo wave function that matches the node-less wave function with value and derivative, as well as with value and derivative of $\hat{t}\phi$.

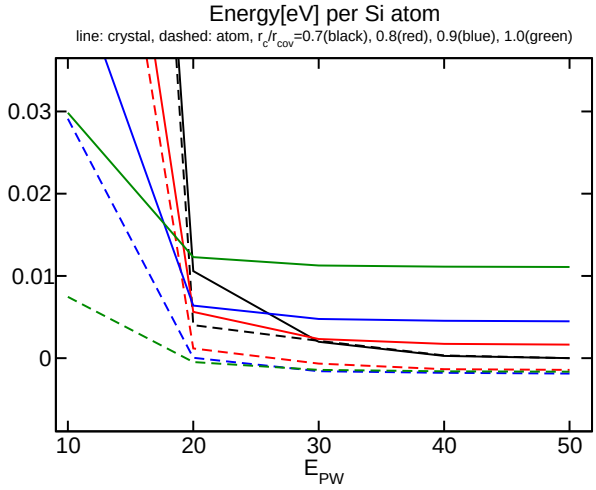

Fig. 1.1: Plane wave convergence of the energy of silicon crystal (full) and a silicon atom (dashed) for different radii in the augmentation with type 'ndlss'. A cutoff of $0.7r_{cov}$ seems to be the best choice. The energies are relative to the result for $r_c = 0.7r_{cov}$ and $E_{PW} = 50$ Ry. Given that we will use a plane wave cutoff of 30Ry for most calculations an augmentation radius of 0.7-0.8 r_{cov} appears to be the best choice.

1.2 Relativistic effects

I recommend to read the doctoral thesis entitled "The ZORA equation" of Eric van Lenthe[2], if you can get your hands on it.

1.2.1 Dirac equation

We start from the Dirac equation of an electron in an electric field. First we divide the four-component wave function into an upper part $\phi = (\Psi_1, \Psi_2)$ and a lower part $\chi = (\Psi_3, \Psi_4)$

$$\begin{pmatrix} v-\epsilon & \vec{\sigma}\vec{p}c \\ \vec{\sigma}\vec{p}c & -2m_0c^2+v-\epsilon \end{pmatrix} \begin{pmatrix} |\phi\rangle \\ |\chi\rangle \end{pmatrix} = 0 \tag{1.41}$$

where ϵ is the energy of the electron relative to the rest-energy m_0c^2. $\vec{\sigma}$ is a vector of 2×2 matrices formed from the three Pauli matrices $\sigma_x, \sigma_y, \sigma_z$.

It will be convenient to introduce the function

$$1 + D(\vec{r}) \stackrel{\text{def}}{=} \left[1 + \frac{\epsilon - v(\vec{r})}{2m_0c^2}\right]^{-1} \tag{1.42}$$

so that the Dirac equation obtains the form

$$\begin{pmatrix} v-\epsilon & \vec{\sigma}\vec{p}c \\ \vec{\sigma}\vec{p}c & \frac{-2m_0c^2}{1+D} \end{pmatrix} \begin{pmatrix} |\phi\rangle \\ |\chi\rangle \end{pmatrix} = 0 \tag{1.43}$$

The small contribution can be extracted from the second equation of Eq. 1.43

$$|\chi\rangle = \frac{1}{2m_0c^2+\epsilon-v}\vec{\sigma}\vec{p}c|\phi\rangle = \frac{1+D}{2m_0c}\vec{\sigma}\vec{p}|\phi\rangle \tag{1.44}$$

Thus, the small component can be eliminated from the first equation of Eq. 1.43, which is turned into a second-order differential equation for the large component.

$$\left[\vec{\sigma}\vec{p}\frac{1+D}{2m_0}\vec{\sigma}\vec{p} + v - \epsilon\right]|\phi\rangle = 0 \tag{1.45}$$

Using the magic equation

$$(\vec{\sigma}\vec{a})(\vec{\sigma}\vec{b}) = \vec{a}\vec{b} + i\vec{\sigma}(\vec{a}\times\vec{b}) \tag{1.46}$$

we obtain the form

$$\begin{aligned} \left[\vec{p}\frac{1+D}{2m_0}\vec{p} + i\vec{\sigma}\left(\vec{p}\frac{1+D}{2m_0}\times\vec{p}\right) + v - \epsilon\right]|\phi\rangle = 0 \\ \left[\frac{1+D}{2m_0}\vec{p}^2 - i\frac{\hbar}{2m_0}(\vec{\nabla}D)\vec{p} + \vec{S}\left(\frac{\vec{\nabla}D}{m_0}\times\vec{p}\right) + v - \epsilon\right]|\phi\rangle = 0 \end{aligned} \tag{1.47}$$

where $\vec{S} = \frac{\hbar}{2}\vec{\sigma}$ is the spin. For a rotationally symmetric $D(\vec{r})$, we can introduce the orbit angular momentum $\vec{L} = \vec{r} \times \vec{p}$ and we obtain the Dirac equation in the form

$$\begin{aligned}\Big[\frac{1+D}{2m_0}\vec{p}^2 - i\frac{\hbar\partial_r D}{2m_0|\vec{r}|}\vec{r}\vec{p} + i\frac{2}{\hbar}\vec{S}\Big(\frac{\hbar}{i}(\underbrace{\vec{\nabla}\frac{1+D}{2m_0}}_{\frac{(\partial_r D)}{2m_0}\frac{\vec{r}}{|\vec{r}|}} \times\vec{p}\Big) + v - \epsilon\Big]|\phi\rangle = 0 \\ \Rightarrow \Big[\frac{1+D}{2m_0}\vec{p}^2 - i\frac{\hbar\partial_r D}{2m_0|\vec{r}|}\vec{r}\vec{p} + \underbrace{\frac{(\partial_r D)}{m_0|\vec{r}|}\vec{S}\vec{L}}_{\text{spin-orbit}} + v - \epsilon\Big]|\phi\rangle = 0\end{aligned} \tag{1.48}$$

1.2.2 Approximation

Norm and overlap operator

The Dirac equation is a differential equation with an energy-dependent differential operator.

$$\hat{K}(\epsilon)|\phi\rangle = 0 \tag{1.49}$$

For a given energy ϵ_0 the differential operator can be linearized in energy yielding

$$\Big[\hat{h} - \epsilon\hat{o}\Big]|\phi\rangle = O\Big((\epsilon - \epsilon_0)^2\Big) \tag{1.50}$$

with

$$\begin{aligned}\hat{h} &:= \hat{K}(\epsilon_0) - \left.\frac{d\hat{K}}{d\epsilon}\right|_{\epsilon_0}\epsilon_0 \\ \hat{o} &:= -\left.\frac{d\hat{K}}{d\epsilon}\right|_{\epsilon_0}\end{aligned} \tag{1.51}$$

For the Dirac equation Eq. 1.41, the overlap operator has the form

$$\hat{o} = \begin{pmatrix}\mathbf{1} & \mathbf{0}\\ \mathbf{0} & \mathbf{1}\end{pmatrix} \tag{1.52}$$

which is the well-known norm condition.

In the following we will introduce approximations by changing the relativistic factor. The rule given above provides us with guidance, how the small component is to be treated.

The same procedure, applied to the two-component equation yields the normalization equation for the large component: I start from Eq. 1.45

$$\begin{aligned}\hat{K}(\epsilon) &= \vec{\sigma}\vec{p}\frac{1+D}{2m_0}\vec{\sigma}\vec{p} + v - \epsilon \\ -\partial_\epsilon\hat{K}(\epsilon) &\overset{\text{Eq. } 1.42}{=} 1 + \vec{\sigma}\vec{p}\Big(\frac{1+D}{2m_0 c}\Big)^2\vec{\sigma}\vec{p}\end{aligned} \tag{1.53}$$

Thus the overlap can be obtained by constructing the small component using the second form of Eq. 1.44 and then to form the squares.

This suggests that the small component shall be set to zero, whenever, a energy-independent relativistic factor is chosen.

Specific approximations

- non-relativistic approximation: We keep the terms of zero'th order in $\frac{|\vec{p}|}{c}$, respectively $\frac{\epsilon - v}{m_0 c^2}$. This amounts to (1) setting the relativistic factor $D(r)$ equal to zero. Following the argument given above, also the small component is set to zero. Thus we obtain the Pauli equation, which separates into two Schrödinger equations.

$$\Big[\frac{\vec{p}^2}{2m_0} + v - \epsilon\Big]|\phi\rangle = 0 \qquad \text{with} \qquad |\chi\rangle = 0 \tag{1.54}$$

- The ZORA (Zero'th Order Relativistic Approximation): The relativistic factor $D^Z(r) = D(\bar{\epsilon}(r), r)$ is kept an energy independent function of position.

$$\Big[\frac{1 + D^Z}{2m_0}\vec{p}^2 - i\frac{\hbar\partial_r D^Z}{2m_0|\vec{r}|}\vec{r}\vec{p} + \underbrace{\frac{(\partial_r D^Z)}{m_0|\vec{r}|}\vec{S}\vec{L}}_{\text{spin-orbit}} + v - \epsilon\Big]|\phi\rangle = 0 \qquad \text{with} \qquad |\chi\rangle = 0 \tag{1.55}$$

- The FORA (First-Order Relativistic Approximation): The relativistic factor $D(r)$ is kept a function

$$D^F(\epsilon, r) = D(\bar{\epsilon}(r), r)) + \Big(\epsilon - \bar{\epsilon}(r)\Big)\,\partial_\epsilon D(\epsilon, r)|_{\epsilon=\bar{\epsilon}(r)} \tag{1.56}$$

  of position, which is linear in the density.

$$\Big[\frac{1 + D^F(\epsilon)}{2m_0}\vec{p}^2 - i\frac{\hbar\partial_r D^F(\epsilon)}{2m_0|\vec{r}|}\vec{r}\vec{p} + \underbrace{\frac{(\partial_r D^F(\epsilon))}{m_0|\vec{r}|}\vec{S}\vec{L}}_{\text{spin-orbit}} + v - \epsilon\Big]|\phi\rangle = 0$$

$$|\chi\rangle = \frac{1 + D^F(\epsilon, r)}{2m_0 c^2}\vec{\sigma}\vec{p}|\phi\rangle \tag{1.57}$$

- The complete relativistic description uses the original relativistic factor without approximation.

The second type of approximation is the scalar relativistic approximation. The scalar relativistic approximation is automatically included in the non-relativistic derscription, it is optional in ZORA and it is incompatible with FORA and a full relativistic description.

Note that we treat the Term ZORA more flexible that the common usage in the literature, because we allow for an arbitrary choice of $\bar{\epsilon}$.

- the common ZORA uses $\bar{\epsilon} = 0$
- the non-relativistic approximation uses $\bar{\epsilon} = v(r)$

I recommend the choice (not implemented...)

$$\bar{\epsilon}(\vec{r}) = \max\Big[v(r), \frac{\sum_n f_n|\phi_n(r)|^2\epsilon_n}{\sum_n f_n|\phi_n(r)|^2}\Big] \tag{1.58}$$

This choice ensures that from a certain radius outward, the relativistic effects are suppressed completely.

1.2.3 Relativistic augmentation

It is our goal to separate all relativistic effects out into the augmentation contribution, so that we need not consider the relativistic effects in the plane-wave part. The plane-wave part does not involve large kinetic energies so that their contribution to the relativistic effects can be ignored with good confidence.

In the PAW method, we make the following Ansatz for the wave function:

$$\begin{pmatrix} |\phi\rangle \\ |\chi\rangle \end{pmatrix} = \begin{pmatrix} |\tilde{\psi}\rangle \\ \frac{1}{2m_0c}\vec{\sigma}\vec{p}|\tilde{\psi}\rangle \end{pmatrix} + \sum_\alpha \left[\begin{pmatrix} |\phi_\alpha\rangle \\ \frac{1+D}{2m_0c}\vec{\sigma}\vec{p}|\phi_\alpha\rangle \end{pmatrix} - \begin{pmatrix} |\tilde{\phi}_\alpha\rangle \\ \frac{1}{2m_0c}\vec{\sigma}\vec{p}|\tilde{\phi}_\alpha\rangle \end{pmatrix} \right] \langle \tilde{p}_\alpha|\tilde{\psi}\rangle \tag{1.59}$$

This ansatz ensures that the wave function is continuous–if $D(r)$ vanishes smoothly beyond the augmentation radius–and that all-electron and pseudo partial waves become identical.

This mapping from a two-dimensional Pauli spinor onto a four component spinor wave function is reminiscent of the Foldy-Wouthuysen transformation[3], which diagonalizes the matrix form of the Dirac Hamiltonian.[2]

$$\begin{pmatrix} \langle\phi| \\ \langle\chi| \end{pmatrix} \begin{pmatrix} v-\epsilon & (\vec{\sigma}\vec{p}c)^\dagger \\ \vec{\sigma}\vec{p}c & -2m_0c^2+v-\epsilon \end{pmatrix} \begin{pmatrix} |\phi\rangle \\ |\chi\rangle \end{pmatrix} = 0 \tag{1.60}$$

For the pseudo contribution, we change the all-electron potential to the pseudo potential $\tilde{v}$ and we set the relativistic factor D to zero.

In addition we introduce the small components of the partial waves

$$\begin{aligned} |\chi_\alpha\rangle &= (1+D_\alpha)\frac{\vec{\sigma}\vec{p}}{2m_0c}|\phi_\alpha\rangle \\ |\tilde{\chi}_\alpha\rangle &= \frac{\vec{\sigma}\vec{p}}{2m_0c}|\tilde{\phi}_\alpha\rangle \end{aligned} \tag{1.61}$$

The index on the D_α indicates that it has been evaluated with the energy ϵ_α, the energy used in the nodeless equation for $|\phi_\alpha\rangle$.

For the small pseudo partial wave we made the choice to set D to zero, while we keep the finite speed of light.

To extract Hamiltonian and Overlap operator from the Dirac equation, I form the matrix

[2] Here we distinguish $\vec{\sigma}\vec{p}$ and its hermitean conjugate $(\vec{\sigma}\vec{p})^\dagger$. This refers to the fact that the identity is not valid on a point-per-point basis, but only in connection with certain boundary conditions.

element of the Dirac equation with the corresponding Bra.

$$
\begin{aligned}
\Rightarrow 0 = &\begin{pmatrix} \langle\tilde{\psi}| \\ \langle\tilde{\psi}|\frac{(\vec{\sigma}\vec{p})^\dagger}{2m_0c} \end{pmatrix} \begin{pmatrix} \tilde{v}-\epsilon & (\vec{\sigma}\vec{p}c)^\dagger \\ \vec{\sigma}\vec{p}c & -2m_0c^2+\tilde{v}-\epsilon \end{pmatrix} \begin{pmatrix} |\psi\rangle \\ \frac{\vec{\sigma}\vec{p}}{2m_0c}|\tilde{\psi}\rangle \end{pmatrix} \\
&+\sum_{\alpha,\beta}\langle\tilde{\psi}|\tilde{p}_\alpha\rangle\left[\begin{pmatrix} \langle\phi_\alpha| \\ \langle\chi_\alpha| \end{pmatrix} \begin{pmatrix} v-\epsilon & (\vec{\sigma}\vec{p}c)^\dagger \\ \vec{\sigma}\vec{p}c & -2m_0c^2+v-\epsilon \end{pmatrix} \begin{pmatrix} |\phi_\beta\rangle \\ |\chi_\beta\rangle \end{pmatrix}\right. \\
&\qquad\left.-\begin{pmatrix} \langle\tilde{\phi}_\alpha| \\ \langle\tilde{\chi}_\alpha| \end{pmatrix} \begin{pmatrix} \tilde{v}-\epsilon & (\vec{\sigma}\vec{p}c)^\dagger \\ \vec{\sigma}\vec{p}c & -2m_0c^2+\tilde{v}-\epsilon \end{pmatrix} \begin{pmatrix} |\tilde{\phi}_\beta\rangle \\ |\tilde{\chi}_\beta\rangle \end{pmatrix}\right]\langle\tilde{p}_\beta|\tilde{\psi}\rangle \\
&=\langle\tilde{\psi}|\frac{\hat{\vec{p}}^2}{2m_0}+\tilde{v}-\epsilon+\underbrace{(\vec{\sigma}\vec{p})^\dagger\frac{(\tilde{v}-\epsilon)}{(2m_0c)^2}(\vec{\sigma}\vec{p})}_{\text{ignored}}|\tilde{\psi}\rangle \\
&+\sum_{\alpha,\beta}\langle\tilde{\psi}|\tilde{p}_\alpha\rangle\Big\{\underbrace{\Big[\overbrace{\langle\phi_\alpha|}^{\langle\chi_\alpha|}(\vec{\sigma}\vec{p})^\dagger\frac{1+D_\alpha}{2m_0}(\vec{\sigma}\vec{p})|\phi_\beta\rangle+\langle\phi_\alpha|(\vec{\sigma}\vec{p})^\dagger\overbrace{\frac{1+D_\beta}{2m_0}(\vec{\sigma}\vec{p})|\phi_\beta\rangle}^{|\chi_\beta\rangle}-2m_0c^2\langle\chi_\alpha|\chi_\beta\rangle\Big]}_{T_{\alpha,\beta}} \\
&\qquad-\underbrace{\Big[\overbrace{\langle\tilde{\phi}_\alpha|}^{\langle\tilde{\chi}_\alpha|}(\vec{\sigma}\vec{p})^\dagger\frac{1}{2m_0}(\vec{\sigma}\vec{p})+(\vec{\sigma}\vec{p})^\dagger\overbrace{\frac{1}{2m_0}(\vec{\sigma}\vec{p})|\tilde{\phi}_\beta\rangle}^{|\tilde{\chi}_\beta\rangle}-2m_0c^2\langle\tilde{\chi}_\alpha|\tilde{\chi}_\beta\rangle\Big]}_{\tilde{T}_{\alpha,\beta}} \\
&\qquad+\langle\phi_\alpha|v-\epsilon|\phi_\beta\rangle+\langle\chi_\alpha|v-\epsilon|\chi_\beta\rangle-\langle\tilde{\phi}_\alpha|\tilde{v}-\epsilon|\tilde{\phi}_\beta\rangle-\langle\tilde{\chi}_\alpha|\tilde{v}-\epsilon|\tilde{\chi}_\beta\rangle\Big\}\langle\tilde{p}_\beta|\tilde{\psi}\rangle
\end{aligned}
\tag{1.62}
$$

We used that $(\vec{\sigma}\vec{p})^2=\vec{p}^2$.

The three terms marked in red are problematic, because the first one contributes to plane wave part. The all-electron term is not neglegible in the core region, but it also does not vanish in the tail region, if the partial waves, and with it their small components, diverge with increasing radius. This diverging part does, however, not contribute, because it is cancelled by the corresponding one-center pseudo term. This is also the reason that the pseudo term needs to be included.

1.2.4 Approximation of relativistic effects for the PAW-Hamiltonian

The pseudo term of the plane wave part marked in red

$$
\begin{aligned}
\langle\tilde{\psi}|(\vec{\sigma}\vec{p})\frac{(\tilde{v}-\epsilon)}{(2m_0c)^2}(\vec{\sigma}\vec{p})|\tilde{\psi}\rangle &= \langle\tilde{\psi}|\frac{1}{(2m_0c)^2}\frac{\hbar}{i}(\vec{\nabla}\tilde{v})\vec{p}+\frac{2}{(2m_0c)^2}\vec{S}\Big((\vec{\nabla}\tilde{v})\times\vec{p}\Big)+\frac{(\tilde{v}-\epsilon)}{c^2}\frac{\vec{p}^2}{2m_0}|\tilde{\psi}\rangle \\
&= \frac{1}{2m_0c^2}\langle\tilde{\psi}|\frac{-i\hbar}{2m_0}(\vec{\nabla}\tilde{v})\vec{p}+\frac{1}{m_0}\vec{S}\Big((\vec{\nabla}\tilde{v})\times\vec{p}\Big)+(\tilde{v}-\epsilon)\vec{p}^2|\tilde{\psi}\rangle
\end{aligned}
\tag{1.63}
$$

is considered to be small and is ignored in the current implementation. Let us investigate the size of the error.

In order to estimate its size let us consider the free electron case, where the wave functions are simple plane waves.

$$\langle\tilde{\psi}|(\vec{\sigma}\vec{p})\frac{(\tilde{v}-\epsilon)}{(2m_0c)^2}(\vec{\sigma}\vec{p})|\tilde{\psi}\rangle = \frac{(\hbar\vec{G})^2}{2m_0}\frac{\epsilon-v}{2m_0c^2} \approx \frac{E_{kin}^2}{2m_0c^2} \approx E_{kin}^2\cdot 2.5\times10^{-5}\frac{1}{H}$$
$$\approx \begin{cases} 5.00mH\cdot N_e & \text{for } E_{kin}=30 \text{ Ry} \\ 0.60mH\cdot N_e & \text{for } E_{kin}=10 \text{ Ry} \\ 0.06mH\cdot N_e & \text{for } E_{kin}=5 \text{ Ry} \end{cases}$$

where N_e is the number of electrons.

Alternatives: Conceivable is to remove the first term from the pseudo one-center part along with ignoring the complete plane wave part of the small component. The rational is that this term captures the dominant term of the pseudo plane wave part, while it does not have the exponentially increasing behavior that needs to be canceled in the all-electron term.

1.2.5 Relativistic PAW-Hamiltonian

With the neglect of the term Eq. 1.63, we obtain

$$\begin{aligned}
0 &= \langle\tilde{\Psi}|\hat{\tilde{H}}-\hat{\tilde{O}}\epsilon|\tilde{\Psi}\rangle \\
&= \langle\tilde{\psi}|\frac{\hat{\tilde{p}}^2}{2m_0}+\tilde{v}-\epsilon+\sum_{\alpha,\beta}|\tilde{p}_\alpha\rangle\Big(dT_{\alpha,\beta}+dV_{\alpha,\beta}-\epsilon dO_{\alpha,\beta}\Big)\langle\tilde{p}_\beta||\tilde{\psi}\rangle \\
&= \langle\tilde{\psi}|\frac{\hat{\tilde{p}}^2}{2m_0}+\tilde{v}-\epsilon|\tilde{\psi}\rangle \\
&+\sum_{\alpha,\beta}\langle\tilde{\psi}|\tilde{p}_\alpha\rangle\Bigg\{\underbrace{\Big[\overbrace{\langle\phi_\alpha|(\vec{\sigma}\vec{p})^\dagger\frac{1+D_\alpha}{2m_0}}^{\langle\chi_\alpha|}(\vec{\sigma}\vec{p})|\phi_\beta\rangle+\langle\phi_\alpha|(\vec{\sigma}\vec{p})^\dagger\overbrace{\frac{1+D_\beta}{2m_0}(\vec{\sigma}\vec{p})|\phi_\beta\rangle}^{|\chi_\beta\rangle}-2m_0c^2\langle\chi_\alpha|\chi_\beta\rangle\Big]}_{T_{\alpha,\beta}} \\
&\quad\underbrace{-\Big[\overbrace{\langle\tilde{\phi}_\alpha|(\vec{\sigma}\vec{p})^\dagger\frac{1}{2m_0}}^{\langle\tilde{\chi}_\alpha|}(\vec{\sigma}\vec{p})+(\vec{\sigma}\vec{p})^\dagger\overbrace{\frac{1}{2m_0}(\vec{\sigma}\vec{p})|\tilde{\phi}_\beta\rangle}^{|\tilde{\chi}_\beta\rangle}-2m_0c^2\langle\tilde{\chi}_\alpha|\tilde{\chi}_\beta\rangle\Big]}_{\tilde{T}_{\alpha,\beta}} \\
&\quad+\langle\phi_\alpha|v-\epsilon|\phi_\beta\rangle+\langle\chi_\alpha|v-\epsilon|\chi_\beta\rangle-\langle\tilde{\phi}_\alpha|\tilde{v}-\epsilon|\tilde{\phi}_\beta\rangle-\langle\tilde{\chi}_\alpha|\tilde{v}-\epsilon|\tilde{\chi}_\beta\rangle\Bigg\}\langle\tilde{p}_\beta|\tilde{\psi}\rangle
\end{aligned} \tag{1.64}$$

- Thus we obtain pseudo kinetic energy operator as

$$\begin{aligned}\hat{\tilde{T}} &= \frac{\hat{\tilde{p}}^2}{2m_0} + \sum_{\alpha,\beta} |\tilde{p}_\alpha\rangle dT_{\alpha,\beta} \langle\tilde{p}_\beta| \\ dT_{\alpha,\beta} &= \underbrace{\langle\phi_\alpha|(\vec{\sigma}\vec{p})\frac{1+D_\alpha}{2m_0}(\vec{\sigma}\vec{p})}_{\langle g_\alpha| - \langle\phi_\alpha|(v-\epsilon_\alpha)} |\phi_\beta\rangle + \langle\phi_\alpha| \underbrace{(\vec{\sigma}\vec{p})\frac{1+D_\beta}{2m_0}(\vec{\sigma}\vec{p})|\phi_\beta\rangle}_{|g_\beta\rangle - (v-\epsilon_\beta)|\phi_\beta\rangle} - 2m_0c^2\langle\chi_\alpha|\chi_\beta\rangle \\ &- \underbrace{\langle\tilde{\phi}_\alpha|\frac{\hat{\tilde{p}}^2}{2m_0}}_{\langle\tilde{g}_\alpha| - \langle\tilde{\phi}_\alpha|(\tilde{v}-\epsilon_\alpha)} |\tilde{\phi}_\beta\rangle - \langle\tilde{\phi}_\alpha| \underbrace{\frac{\hat{\tilde{p}}^2}{2m_0}|\tilde{\phi}_\beta\rangle}_{|\tilde{g}_\beta\rangle - (\tilde{v}-\epsilon_\beta)|\tilde{\phi}_\beta\rangle} + 2m_0c^2\langle\tilde{\chi}_\alpha|\tilde{\chi}_\beta\rangle\end{aligned} \tag{1.65}$$

  Here we exploit that the partial waves are constructed from a radial Dirac equation of the form

$$\begin{aligned}\left[(\vec{\sigma}\vec{p})\frac{1+D_\beta}{2m_0}(\vec{\sigma}\vec{p}) + v - \epsilon_\beta\right]|\phi_\beta\rangle &= |g_\beta\rangle \\ \left[\frac{\hat{\tilde{p}}^2}{2m_0} + \tilde{v} - \epsilon_\beta\right]|\tilde{\phi}_\beta\rangle &= |\tilde{g}_\beta\rangle\end{aligned} \tag{1.66}$$

- The relativistic pseudo overlap operator has the form

$$\begin{aligned}\hat{\tilde{O}} &= 1 + \sum_{\alpha,\beta} |\tilde{p}_\alpha\rangle dO_{\alpha,\beta} \langle\tilde{p}_\beta| \\ dO_{\alpha,\beta} &= \langle\phi_\alpha|\phi_\beta\rangle + \langle\chi_\alpha|\chi_\beta\rangle - \langle\tilde{\phi}_\alpha|\tilde{\phi}_\beta\rangle - \langle\tilde{\chi}_\alpha|\tilde{\chi}_\beta\rangle\end{aligned} \tag{1.67}$$

- The potential energy has the form

$$\begin{aligned}\hat{\tilde{v}} &= \hat{v} + \sum_{\alpha,\beta} |\tilde{p}_\alpha\rangle dV_{\alpha,\beta} \langle\tilde{p}_\beta| \\ dV_{\alpha,\beta} &= \langle\phi_\alpha|\hat{v}|\phi_\beta\rangle + \langle\chi_\alpha|\hat{v}|\chi_\beta\rangle - \langle\tilde{\phi}_\alpha|\tilde{v}|\tilde{\phi}_\beta\rangle - \langle\tilde{\chi}_\alpha|\tilde{v}|\tilde{\chi}_\beta\rangle\end{aligned} \tag{1.68}$$

  From the expression of the potential energy, we obtain a representation for the density, namely

$$\begin{aligned}n(\vec{r}) = \underbrace{\sum_n f_n \tilde{\psi}_n^2(\vec{r}) + \tilde{n}_c}_{\tilde{n}(\vec{r})} &+ \underbrace{\sum_{\alpha,\beta} \theta_{\alpha,\beta}\left(\phi_\beta^*(\vec{r})\phi_\alpha^*(\vec{r}) + \chi_\beta^*(\vec{r})\chi_\alpha^*(\vec{r})\right) + n_c(\vec{r})}_{n^1(\vec{r})} \\ &- \underbrace{\sum_{\alpha,\beta} \theta_{\alpha,\beta}\left(\tilde{\phi}_\beta^*(\vec{r})\tilde{\phi}_\alpha^*(\vec{r}) + \tilde{\chi}_\beta^*(\vec{r})\tilde{\chi}_\alpha^*(\vec{r})\right) + \tilde{n}_c(\vec{r})}_{\tilde{n}^1(\vec{r})}\end{aligned} \tag{1.69}$$

  Here $n_c(\vec{r})$ is the core electron density and $\tilde{n}_c(\vec{r})$ is the core pseudo electron density.

  The one-center density matrix $\theta_{\alpha,\beta}$ is defined as

$$\theta_{\alpha,\beta} = \sum_n \langle\tilde{p}_\alpha|\tilde{\psi}_n\rangle f_n \langle\tilde{p}_\beta\rangle \tag{1.70}$$

1.2.6 Nodeless construction for the Dirac equation

We generalize Eq. 1.3 to the Dirac equation, which yields

$$\begin{pmatrix} v-\epsilon_n & \vec{\sigma}\vec{p}c \\ \vec{\sigma}\vec{p}c & -2m_0c^2+v-\epsilon_n \end{pmatrix} \begin{pmatrix} |u_n\rangle \\ |v_n\rangle \end{pmatrix} = - \begin{pmatrix} |u_{n-1}\rangle \\ |v_{n-1}\rangle \end{pmatrix} \tag{1.71}$$

where the small component of a nodeless function is denoted by $|v_n\rangle$.

We resolve for the small component $|v_n\rangle$

$$|v_n\rangle = \frac{1+D_n}{2m_0c}(\vec{\sigma}\vec{p})|u_n\rangle + \frac{1+D_n}{2m_0c^2}|v_{n-1}\rangle \tag{1.72}$$

and insert the result into the first equation

$$\begin{aligned} (v-\epsilon)|u_n\rangle + (\vec{\sigma}\vec{p})c|v_n\rangle &= -|u_{n-1}\rangle \\ \Big[(\vec{\sigma}\vec{p})\frac{1+D_n}{2m_0}(\vec{\sigma}\vec{p}) + v - \epsilon_n\Big]|u_n\rangle &= -|u_{n-1}\rangle - (\vec{\sigma}\vec{p})\frac{1+D_n}{2m_0c}|v_{n-1}\rangle \\ \Big[(1+D_n)\frac{\vec{p}^2}{2m_0} + \frac{\hbar}{i}\frac{\vec{\nabla}D_n}{2m_0}\vec{p} + \vec{S}\Big(\frac{\vec{\nabla}D_n}{m_0}\times\vec{p}\Big) + v - \epsilon_n\Big]|u_n\rangle &= -|u_{n-1}\rangle - (\vec{S}\vec{p})\frac{1+D_n}{\hbar m_0c}|v_{n-1}\rangle \end{aligned} \tag{1.73}$$

1.2.7 Spinor harmonics

For a spherical atom, the spin and orbit angular momenta are no more conserved independently, but only the total angular momentum is conserved. Therefore we need to introduce spinor harmonics.

The spinor harmonics obey the eigenvalue equations

$$\Big(\hat{\vec{L}}+\hat{\vec{S}}\Big)^2|\chi_{\kappa,j_z}\rangle = |\chi_{\kappa,j_z}\rangle \quad \underbrace{\hbar^2(\kappa^2-\frac{1}{2})}_{\hbar^2 j(j+1)} \tag{1.74}$$

$$\hat{\vec{L}}^2|\chi_{\kappa,j_z}\rangle = |\chi_{\kappa,j_z}\rangle \quad \hbar^2\kappa(\kappa+1) \tag{1.75}$$

$$\hat{\vec{S}}^2|\chi_{\kappa,j_z}\rangle = |\chi_{\kappa,j_z}\rangle \quad \hbar^2\frac{3}{4} \tag{1.76}$$

$$\hat{\vec{L}}\hat{\vec{S}}|\chi_{\kappa,j_z}\rangle = |\chi_{\kappa,j_z}\rangle \quad \left(-\hbar^2\frac{\kappa+1}{2}\right) \tag{1.77}$$

$$\left(\hat{L}_z+\hat{S}_z\right)|\chi_{\kappa,j_z}\rangle = |\chi_{\kappa,j_z}\rangle \quad \hbar j_z \tag{1.78}$$

$$\frac{1}{|\vec{r}|}\vec{r}\,\vec{\sigma}\chi_{\kappa,j_z} = -\chi_{-\kappa,j_z} \tag{1.79}$$

where the quantum numbers κ can assume any integer value except zero.

$$\kappa = \ldots, -2, -1, \qquad 1, 2, \ldots \tag{1.80}$$

$$j_z = -|\kappa| + \frac{1}{2}, -|\kappa| + \frac{3}{2}, \ldots, |\kappa| - \frac{1}{2} \tag{1.81}$$

$$j = |\kappa| - \frac{1}{2} \tag{1.82}$$

$$\ell = |\kappa + \frac{1}{2}| - \frac{1}{2} \tag{1.83}$$

$$\begin{pmatrix} m_\uparrow \\ m_\downarrow \end{pmatrix} = \begin{pmatrix} j_z - \frac{1}{2} \\ j_z + \frac{1}{2} \end{pmatrix} \tag{1.84}$$

Furthermore,

$$\vec{L}\vec{S} \begin{cases} < 0 & \text{for } \kappa > 0 \\ = 0 & \text{for } \kappa = -1, \text{ i.e. for } \ell = 0 \\ > 0 & \text{for } \kappa < -1 \end{cases} \tag{1.85}$$

κ	-4	-3	-2	-1	-	1	2	3
ℓ	3	2	1	0	-	1	2	3
ℓ	f	d	p	s	-	p	d	f

The spinor harmonics have the form

$$|\chi_{\kappa,j_z}\rangle \overset{\kappa\leq 0}{=} \begin{pmatrix} |Y_{-\kappa-1,j_z-\frac{1}{2}}\rangle \sqrt{\frac{-\kappa+j_z-\frac{1}{2}}{-2\kappa-1}} \\ |Y_{-\kappa-1,j_z+\frac{1}{2}}\rangle \sqrt{\frac{-\kappa-j_z-\frac{1}{2}}{-2\kappa-1}} \end{pmatrix} \qquad |\chi_{\kappa,j_z}\rangle \overset{\kappa>0}{=} \begin{pmatrix} -|Y_{\kappa,j_z-\frac{1}{2}}\rangle \sqrt{\frac{\kappa-j_z+\frac{1}{2}}{2\kappa+1}} \\ |Y_{\kappa,j_z+\frac{1}{2}}\rangle \sqrt{\frac{\kappa+j_z+\frac{1}{2}}{2\kappa+1}} \end{pmatrix} \tag{1.86}$$

$$\underbrace{\chi_{-\ell-1,m+\frac{1}{2}}}_{\Omega_{\ell+\frac{1}{2},\ell,m+\frac{1}{2}}} = \begin{pmatrix} |Y_{\ell,m}\rangle \sqrt{\frac{\ell+m+1}{2\ell+1}} \\ |Y_{\ell,m+1}\rangle \sqrt{\frac{\ell-m}{2\ell+1}} \end{pmatrix} \qquad \underbrace{\chi_{\ell,m+\frac{1}{2}}}_{\Omega_{\ell-\frac{1}{2},\ell,m+\frac{1}{2}}} = \begin{pmatrix} -|Y_{\ell,m}\rangle \sqrt{\frac{\ell-m}{2\ell+1}} \\ |Y_{\ell,m+1}\rangle \sqrt{\frac{\ell+m+1}{2\ell+1}} \end{pmatrix} \tag{1.87}$$

Then spinor harmonics describe states with the spin parallel or antiparallel to the orbit angular momentum.

1.2.8 Spherical Dirac equations in spinor harmonics

The wave function of an electron is a four-component spinor function consisting of a two-dimensional large and a two-dimensional small component. Each has again a spin-up and a spin-down component.

$$\begin{pmatrix} \phi(\epsilon, \vec{r}) \\ \chi(\epsilon, \vec{r}) \end{pmatrix} = \begin{pmatrix} g_{\kappa,j_z}(\epsilon, \vec{r}) \chi_{\kappa,j_z}(\vec{r}) \\ i f_{-\kappa,j_z}(\epsilon, \vec{r}) \chi_{-\kappa,j_z}(\vec{r}) \end{pmatrix} \tag{1.88}$$

This Ansatz can be inserted into Eq. 1.73 and Eq. 1.72

$$\left[(1+D_n)\frac{\vec{p}^2}{2m_0}+\frac{\hbar}{i}\frac{\partial_r D_n}{2m_0|\vec{r}}\vec{r}\vec{p}+\frac{\partial_r D_n}{m_0|\vec{r}|}\vec{S}\underbrace{\left(\vec{r}\times\vec{p}\right)}_{\vec{L}}+v-\epsilon_n\right]|u_n\rangle=-|u_{n-1}\rangle-(\vec{S}\vec{p})\frac{1+D_n}{\hbar m_0 c}|v_{n-1}\rangle$$

$$|v_n\rangle=\frac{1+D_n}{2m_0}\left[\frac{2}{\hbar c}(\vec{S}\vec{p})|u_n\rangle+\frac{1}{c^2}|v_{n-1}\rangle\right] \tag{1.89}$$

which yields with Eq. 1.77

$$\begin{aligned}\left((1+D)\frac{-\hbar^2}{2m_0}\left(\frac{1}{r}\partial_r^2 r-\frac{\ell(\ell+1)}{r^2}\right)-\frac{\hbar^2(\partial_r D)}{2m_0}\left[\partial_r+\frac{\kappa+1}{|\vec{r}|}\right]+v-\epsilon\right)g^{(n)}_{\kappa,j_z}(\epsilon,r)\\ =-g^{(n-1)}_{\kappa,j_z}(\epsilon_{n-1},r)+\frac{\hbar}{c}\left[\partial_r+\frac{-\kappa+1}{|\vec{r}|}\right]\frac{1+D}{2m_0}f^{(n-1)}_{-\kappa,j_z}(\epsilon_{n-1},r)\\ f^{(n)}_{-\kappa,j_Z}(\epsilon,r)=\frac{1+D(\epsilon)}{2m_0}\left(\frac{\hbar}{c}\left[\partial_r+\frac{\kappa+1}{|\vec{r}|}\right]g^{(n)}_{\kappa,j_z}(\epsilon,r)+\frac{1}{c^2}f^{(n-1)}_{-\kappa,j_z}(\epsilon_{n-1},r)\right)\end{aligned} \tag{1.90}$$

Compare with Eq. 5.49-5.51 of the master thesis of Robert Schade[4]. (Note, however, that I changed the sign of f_n relative to that of f_{n-1}, etc. relative to my earlier notes.)

1.3 Pseudization

1.3.1 Pseudization of core density and potential

For an all-electron quantity $f(\vec{r})$ we determine a pseudized quantity $\tilde{f}(\vec{r})$ according to the following procedure.

$$\tilde{f}(r)=\begin{cases}a+br^\lambda+cr^{\lambda+2} & \text{for} \quad r<r_c\\ f(r) & \text{for} \quad r>r_c\end{cases}$$

The parameters a, b and c are determined such that the pseudo quantity $\tilde{f}$ is differentiable.

The construction depends on three parameters:

- $\tilde{v}(r=0)$
- r_c
- λ

1.4 Nucleus with finite size

The nucleus is considered as a homogeneously charged sphere. The volume of the nucleus is proportional to the number of nucleons. This allows to relate the radius directly to the mass of the nucleus.[5, 6]

$$r_{nuc}=\sqrt[3]{\frac{M}{u}}\cdot 1.2\cdot 10^{15}m=\sqrt[3]{\frac{M}{m_e}}\cdot 1.85635065215\cdot 10^{-6}a_0$$

where M is the mass of the nucleus and $u = \frac{1}{12}m(C^{12})$.

The potential of the nucleus is therefore

$$v_{nuc}(r) = \begin{cases} \frac{-Ze^2}{r_{nuc}}\left(\frac{3}{2} - \frac{1}{2}\frac{r^2}{r_{nuc}^2}\right) & \text{for} \qquad r < r_{nuc} \\ \frac{-Ze^2}{r} & \text{for} \qquad r > r_{nuc} \end{cases}$$

1.5 Fock term

We wish to replace part of the exchange correlation potential by the full exchange potential, that is by the Fock operator. We face the problem that, now, there is a fully non-local potential[3] in the Hamiltonian, which makes the radial Schrödinger equation substantially more complex.

The total energy has the form

$$E = E_{GGA}[n] + \alpha\left(-\frac{1}{2}\sum_{n,m,\sigma,\sigma'}\int dr \int dr' \, \frac{e^2\Psi_n^*(\vec{r},\sigma)\Psi_m^*(\vec{r}',\sigma')\Psi_m(\vec{r},\sigma)\Psi_n(\vec{r}',\sigma')}{4\pi\epsilon_0|\vec{r}-\vec{r'}|} - E_{GGA,X}[n]\right)$$

$$n(\vec{r}) = \sum_{n,\sigma}\Psi_n^*(\vec{r},\sigma)\Psi_n(\vec{r},\sigma)$$

We treat each wave function as a Pauli spinor wave function with a spin up and a spin down component. Usually (without spin-orbit coupling) a state has either a pure spin up or a spin down component. The sum over n runs over all electrons. The term $E_{GGA,x}$ is the exchange only contribution to the exchange functional.

Formulate problem in the form h_0, w. etc. Define all variables.

1.5.1 Generalized perturbation theory

While we are able to obtain the solutions of the Schrödinger equation for a spherical, local or semi-local potential efficiently, the solution for a completely non-local potential is cumbersome even if it is spherical. Here we use an iterative approach, which obtains the result from an approximate solution.

The basic idea is inspired by perturbation theory. In contrast to first order perturbation theory however, we do not require that the approximate solution obeys a Schrödinger equation for some kind of local hamiltonian exactly. This makes it more convenient for a self-consistent, iterative procedure.

Probably, it is more related to the Green's function approach.

Our goal is to find a solution for the inhomogeneous Schrödinger equation

$$\left(\hat{h}_0 + \hat{w} - \varepsilon\right)|\phi\rangle = |I\rangle$$

The hamiltonian shall be divided into an approximate hamiltonian $\hat{h}_0$, having a local potential only, and $\hat{w}$ is a correction including the non-local potential.

We start with an approximate solution $|\phi_0\rangle$, and approximate energy ε_0.

$$\begin{aligned} &\left(\hat{h}_0 + \hat{w} - \varepsilon_0 - \delta\varepsilon\right)|\phi_0 + \delta\phi\rangle = |I\rangle \\ \Rightarrow \qquad &\left(\hat{h}_0 + \hat{w} - \varepsilon_0 - \delta\varepsilon\right)|\delta\phi\rangle = -\left(\hat{h}_0 + \hat{w} - \epsilon_0 - \delta\varepsilon\right)|\phi_0\rangle + |I\rangle \end{aligned}$$

[3] The energy for a fully nonlocal potential must be expressed as $\int d^3r \int d^3r' \, \psi^*(\vec{r})v(\vec{r},\vec{r'})\psi(\vec{r})$.

Now we assume that $(\hat{w} - \delta\varepsilon)|\delta\phi\rangle$ is small. We neglect it and arrive at

$$\left(\hat{h}_0 - \varepsilon_0\right)|\delta\phi\rangle = -\left(\hat{h}_0 + \hat{w} - \epsilon_0 - \delta\varepsilon\right)|\phi_0\rangle + |I\rangle$$

The value of $\delta\varepsilon$ is determined by the boundary conditions.

ITERATIVE SOLUTION OF THE SCHRÖDINGER EQUATION

In practice we determine $|\phi'\rangle$ and $|\partial_\epsilon\phi\rangle$ from

$$\begin{aligned}\left(\hat{h}_0 - \varepsilon_0\right)|\phi\prime\rangle &= -\left(\hat{h}_0 + \hat{w} - \varepsilon_0\right)|\phi_0\rangle + |I\rangle\\ \left(\hat{h}_0 - \varepsilon_0\right)|\partial_\epsilon\phi\rangle &= |\phi_0\rangle\\ (\hat{h}_0 - \epsilon_0)|\phi_{hom}\rangle &= 0\end{aligned}$$

We have explicitely also included the homogeneous solution, which may be admixed into the two states $|\phi'\rangle$ and $|\partial_\epsilon\phi\rangle$.
With these objects we can improve our solution

$$|\phi\rangle = |\phi_0\rangle + |\phi'\rangle + |\partial_\epsilon\phi\rangle\delta\epsilon + |\phi_{hom}\rangle\alpha$$

The parameters $\delta\epsilon$ and α are determined according to the boundary conditions: value, derivative at the integration bounds or energy or norm. The new state $|\phi\rangle$ is not yet the correct result, because we neglected second-order terms, but we can use it as new trial solution $|\phi_0\rangle$ in an iterative procedure.

Let us test the result

$$\begin{aligned}&\left(\hat{h}_0 + \hat{w} - \varepsilon_0 - \delta\varepsilon\right)\Big(|\phi_0\rangle + |\phi'\rangle + |\partial_\varepsilon\phi\rangle\delta\varepsilon + |\phi_{hom}\rangle\alpha\Big) - |I\rangle\\ &= \left(\hat{h}_0 + \hat{w} - \varepsilon_0 - \delta\varepsilon\right)|\phi_0\rangle - |I\rangle\\ &+ \underbrace{\left(\hat{h}_0 - \varepsilon_0\right)|\phi'\rangle}_{-(\hat{h}_0+\hat{w}-\epsilon_0)|\phi_0\rangle+|I\rangle} + (\hat{w} - \delta\varepsilon)\,|\phi'\rangle\\ &+ \underbrace{\left(\hat{h}_0 - \varepsilon_0\right)|\partial_\varepsilon\phi\rangle}_{|\phi_0\rangle}\delta\epsilon + (\hat{w} - \delta\varepsilon)\,|\partial_\varepsilon\phi\rangle\delta\epsilon\\ &+ \underbrace{\left(\hat{h}_0 - \varepsilon_0\right)|\phi_{hom}\rangle}_{=0}\alpha + (\hat{w} - \delta\varepsilon)\,|\phi_{hom}\rangle\alpha\\ &= (\hat{w} - \delta\varepsilon)\Big(|\phi'\rangle + |\partial_\varepsilon\phi\rangle\delta\epsilon + |\phi_{hom}\rangle\alpha\Big)\end{aligned}$$

We can use various boundary conditions: If we set $\delta\varepsilon = 0$ then we obtain a fixed energy solution at $\epsilon = \varepsilon_0$.

On the other hand, we can also adjust $\delta\varepsilon$ to enforce boundary condition at some outer radius. This boundary condition could be that the value at some radius vanishes, or it could be that the solution has a specified logarithmic derivative $D = \partial_r\phi/\phi$ at some radius.

Before we start imposing the boundary conditions we decompose the logarithmic derivative into a value ϕ_0 and a derivative $\partial_r\phi$ at the given radius. These values do not need to be extracted from the initial wave function ϕ_0 used above. We work with value and derivative in order to be

able to deal with infinite logarithmic derivatives, which correspond to the particyularly interesting boundary condition of a hard box.

$$\begin{aligned}
\frac{\partial_r \phi}{\phi} &\stackrel{!}{=} \frac{\partial_r \phi_0}{\phi_0} \\
\frac{\partial_r \phi_0 + \partial_r \phi\prime + \partial_r \partial_\epsilon \phi \delta\epsilon + \partial_r \phi_{hom} \alpha}{\phi_0 + \phi\prime + \partial_\epsilon \phi \delta\epsilon + \phi_{hom}\alpha} &= \frac{\partial_r \phi_0}{\phi_0} \\
\phi_0 \partial_r \phi_0 + \phi_0 \partial_r \phi\prime + \phi_0 \partial_r \partial_\epsilon \phi \delta\epsilon + \phi_0 \partial_r \phi_{hom} \alpha &= \phi_0 \partial_r \phi_0 + \phi\prime \partial_r \phi_0 + \partial_\epsilon \phi \partial_r \phi_0 \delta\epsilon + \phi_{hom} \partial_r \phi_0 \alpha
\end{aligned}$$

With the definition of the **Wronskian**

$$W[f,g] \stackrel{\text{def}}{=} f\partial_r g - g\partial_r f$$

we obtain

$$\begin{aligned}
0 &= W[\phi_0, \phi_0 + \phi'] + W[\phi_0, \partial_\epsilon \phi]\delta\epsilon + W[\phi_0, \phi_{hom}]\alpha \\
\delta\epsilon &= -\frac{W[\phi_0, \phi_0 + \phi']}{W[\phi_0, \partial_\epsilon \phi]} - \frac{W[\phi_0, \phi_{hom}]}{W[\phi_0, \partial_\epsilon \phi]}\alpha
\end{aligned}$$

It is important to resolve the equation for $\delta\epsilon$ because both $W[\phi_0, \phi_0 + \phi']$ and $W[\phi_0, \phi_{hom}]$ approach zero upon convergence, which would create a divide-by-zero.

Thus the solution can be written as

$$|\phi\rangle = \left(|\phi_0\rangle + |\phi'\rangle - |\partial_\epsilon \phi\rangle \frac{W[\phi_0, \phi_0 + \phi']}{W[\phi_0, \partial_\epsilon \phi]}\right) + \left(|\phi_{hom}\rangle - |\partial_\epsilon \phi\rangle \frac{W[\phi_0, \phi_{hom}]}{W[\phi_0, \partial_\epsilon \phi]}\right)\alpha$$

The boundary condition at the outer boundary is fulfilled for any value of α. The value of α is then determined such that the wave function starts with the lowest possible order. The homogeneous solution always starts with r^ℓ. Thus we can only remove that contribution from the inhomogeneous solution.

Relation to nodeless wave functions

We can look upon the nodeless construction in the following way: For each wave function we superimpose the wave functions with less nodes, so that the wave function starts with the lowest possible power.

For our normal Hamiltonian, this implies that the node-less wave function starts as $r^{\ell+2n}$. The Knotensatz garantees that these wave functions are also nodeless (not proven!).

With the Fock term, we can still form wave functions that begin like $r^{\ell+2n}$. We assume here that the radial part of a wave function only contains even orders in its power series expansion, which is a consequence of inversion symmetry (weak argument!). However it is not clear from this argument if the resulting state is also nodeless.

Relation to Greens functions

For the sake of completeness let me show here the relation in terms of Green's functions. This section does not produce funcamentally new insights.

First we define a full Green's function $\hat{G}(\varepsilon)$ and an approximate Green's function $\hat{G}_0(\varepsilon)$ as follows:

$$\begin{aligned}\left(\hat{h}_0 + \hat{w} - \varepsilon\right)\hat{G}(\varepsilon) &= \hat{1}\\ \left(\hat{h}_0 - \varepsilon\right)\hat{G}_0(\varepsilon) &= \hat{1}\end{aligned}$$

Then we express the full Green's function by the approximate one.

$$\begin{aligned}(\hat{G}_0^{-1} + \hat{w})\hat{G} &= \hat{1}\\ (1 + \hat{G}_0\hat{w})\hat{G} &= \hat{G}_0\\ \hat{G} &= \hat{G}_0 - \hat{G}_0\hat{w}\hat{G}\\ \hat{G}^{(n+1)} &= \hat{G}_0 - \hat{G}_0\hat{w}\hat{G}^{(n)}\end{aligned}$$

Here we introduced a series of Green's function, which converges to the full Green's function, if it converges.

The inhomogeneous Schrödinger equation has the form

$$\begin{aligned}|\phi\rangle &= \hat{G}|I\rangle\\ |\phi^{(n+1)}\rangle &= \hat{G}^{(n+1)}|I\rangle\\ &= \left(\hat{G}_0 - \hat{G}_0\hat{w}\hat{G}^{(n)}\right)|I\rangle\\ &= \hat{G}_0|I\rangle - \hat{G}_0\hat{w}|\phi^{(n)}\rangle\\ \hat{G}_0^{-1}\underbrace{\left(|\phi^{(n+1)}\rangle - |\phi^{(n)}\rangle\right)}_{|\delta\phi\rangle} &= |I\rangle - \hat{w}|\phi^{(n)}\rangle + \hat{G}_0^{-1}|\phi^{(n)}\rangle = -\left[\left(\hat{G}_0^{-1} + \hat{w}\right)|\phi^{(n)}\rangle - |I\rangle\right]\\ (\hat{h}_0 - \varepsilon)|\delta\phi\rangle &= -\left[\left(\hat{h}_0 + \hat{w} - \varepsilon\right)|\phi^{(n)}\rangle - |I\rangle\right]\end{aligned}$$

1.5.2 Apply Fock potential to a function

The Fock potential is not yet generalized to include the small component nor spin-orbit coupling.

The Fock operator can be written in the form

$$V_X(\vec{r},\sigma,\vec{r'},\sigma') = -\sum_{j=1}^{N}\frac{e^2\phi_j(\vec{r},\sigma)\phi_j^*(\vec{r'},\sigma')}{4\pi\epsilon_0|\vec{r}-\vec{r'}|}$$

Here $\phi_j(\vec{r},\sigma)$ are spin orbitals. $\sigma \in \{\uparrow,\downarrow\}$. Usually, the wave functions have nonzero elements either for spin up or for spin-down components, but not both.

If there are partially filled angular momentum shells, the occupied and the unoccupied wave functions in the same shell have different shape and energies. Because only the occupied states determine energy and density, we use only the equations for the occupied states.

Now we want to apply this non-local potential to a function $f(\vec{r},\sigma) = f(|\vec{r}|)Y_{L_f}(\vec{r})\delta_{\sigma,\sigma_f}$ with defined angular momentum and s_z character. Thus

$$\begin{aligned}f(\vec{r},\sigma) &= \delta_{\sigma,\sigma_f}f(|\vec{r}|)Y_{L_f}(\vec{r})\\ \phi_j(\vec{r},\sigma) &= \delta_{\sigma,\sigma_j}\phi_j(|\vec{r}|)Y_{L_j}(\vec{r})\\ g(\vec{r},\sigma) &= \delta_{\sigma,\sigma_f}f(|\vec{r}|)Y_{L_f}(\vec{r})\end{aligned}$$

where it needts to be confirmed that g can be represented by a single angular momentum and spin channel.

$$
\begin{aligned}
g(\vec{r},\sigma) &= \sum_{\sigma'} \int d^3r'\, V_X(\vec{r},\sigma,\vec{r'},\sigma') f(\vec{r'},\sigma') \\
&= -\sum_{\sigma'} \int d^3r' \sum_{j=1}^{N} \frac{e^2 \phi_j(\vec{r},\sigma)\phi_j^*(\vec{r'},\sigma')}{4\pi\epsilon_0|\vec{r}-\vec{r'}|} f(\vec{r'},\sigma') \\
&= -\sum_{\sigma'} \sum_{j=1}^{N} \underbrace{\phi_j(|\vec{r}|)Y_{L_j}(\vec{r})\delta_{\sigma,\sigma_j}}_{\phi_j(\vec{r},\sigma)} \int d^3r' \, \frac{e^2}{4\pi\epsilon_0|\vec{r}-\vec{r'}|} \underbrace{\phi_j^*(|\vec{r'}|)Y_{L_j}^*(\vec{r'})\delta_{\sigma',\sigma_j}}_{\phi_j^*(\vec{r'},\sigma')} \underbrace{f(|\vec{r'}|)Y_{L_f}(\vec{r'})\delta_{\sigma',\sigma_f}}_{f(\vec{r'},\sigma')} \\
&= -\sum_{j=1}^{N} \underbrace{\underbrace{\left[\sum_{\sigma'} \delta_{\sigma',\sigma_j}\delta_{\sigma',\sigma_f}\right]}_{\delta_{\sigma_j,\sigma_f}} \delta_{\sigma,\sigma_j}}_{\delta_{\sigma_j,\sigma_f}\delta_{\sigma,\sigma_f}} \phi_j(|\vec{r}|)Y_{L_j}(\vec{r}) \int d^3r' \, \frac{e^2}{4\pi\epsilon_0|\vec{r}-\vec{r'}|} \phi_j(|\vec{r'}|) f(|\vec{r'}|) \underbrace{Y_{L_j}^*(\vec{r'})Y_{L_f}(\vec{r'})}_{\sum_{L_\rho} C^*_{L_f,L_j,L_\rho} Y^*_{L_\rho}(\vec{r'})} \\
&= -\delta_{\sigma,\sigma_f} \sum_{j=1}^{N} \delta_{\sigma_j,\sigma_f} \phi_j(|\vec{r}|)Y_{L_j}(\vec{r}) \sum_{L_\rho} C^*_{L_f,L_j,L_\rho} \int d^3r' \, \frac{e^2}{4\pi\epsilon_0|\vec{r}-\vec{r'}|} \phi_j^*(|\vec{r'}|) f(|\vec{r'}|) Y^*_{L_\rho}(\vec{r'}) \\
&= -\delta_{\sigma,\sigma_f} \sum_{j=1}^{N} \delta_{\sigma_j,\sigma_f} \phi_j(|\vec{r}|)Y_{L_j}(\vec{r}) \sum_{L_\rho} C^*_{L_f,L_j,L_\rho} Y_{L_\rho}(\vec{r}) \\
&\quad \times \underbrace{\int d^3r' \left[Y^*_{L_\rho}(\vec{r'}) \frac{1}{|\vec{r'}|^2} \delta(|\vec{r}|-|\vec{r'}|) \Big[\int d^3r'' \, \frac{e^2}{4\pi\epsilon_0|\vec{r'}-\vec{r''}|} \phi_j(|\vec{r''}|) f(|\vec{r''}|) Y_{L_\rho}(\vec{r''}) \Big] \right]^*}_{=: v^{(j,f)}_{L_\rho}(|\vec{r}|)} \\
&= -\delta_{\sigma,\sigma_f} \sum_{j=1}^{N} \delta_{\sigma_j,\sigma_f} \phi_j(|\vec{r}|) \sum_{L_\rho} C^*_{L_f,L_j,L_\rho} \underbrace{Y_{L_j}(\vec{r})Y^*_{L_\rho}(\vec{r})}_{\sum_{L_g} C_{L_\rho,L_j,L_g} Y_{L_g}} v^{(j,f)}_{L_\rho}(|\vec{r}|) \\
&= -\sum_{L_g} Y_{L_g}(\vec{r})\delta_{\sigma,\sigma_f} \sum_{j=1}^{N} \delta_{\sigma_j,\sigma_f} \sum_{L_\rho} C^*_{L_f,L_j,L_\rho} C_{L_\rho,L_j,L_g} \phi_j^*(|\vec{r}|) v^{(j,f)}_{L_\rho}(|\vec{r}|)
\end{aligned}
$$

where $C_{L,L',L''} := \int d\Omega \, Y^*_L(\vec{r})Y_{L'}(\vec{r})Y_{L''}(\vec{r})$ is the Gaunt coefficient, so that

$$Y^*_L(\vec{r})Y_{L'}(\vec{r}) = \sum_{L''} C_{L,L',L''} Y_{L''}(\vec{r})$$

and the potential is defined as

$$v^{j,f}_{L_\rho}(\vec{r}) = \int d^3r' \, \frac{e^2 \phi_j(|\vec{r'}|) f(|\vec{r'}|) Y_{L_\rho(\vec{r'})}}{4\pi\epsilon_0|\vec{r}-\vec{r'}|}$$

The potential has a pure L_ρ character and is obtained using RADIAL$POISSON.

Furthermore we used the identity

$$\begin{aligned}\int d^3r' \left[Y_L^*(\vec{r'})\frac{1}{|\vec{r'}|^2}\delta(r-|\vec{r'}|)\right]f(\vec{r}) &= \int d^3r' \left[Y_L^*(\vec{r'})\frac{1}{|\vec{r'}|^2}\delta(r-|\vec{r'}|)\right]\left[\sum_{L'} f_{L'}(|\vec{r'}|)Y_{L'}(\vec{r'})\right] \\ &= \sum_{L'} \underbrace{\left[\int d\Omega\, Y_{L'}(\vec{r'})Y_L^*(\vec{r'})\right]}_{\delta_{L,L'}}\left[\int dr'\; r'^2 f'_L(r')\frac{1}{r'^2}\delta(r-r')\right] \\ &= \left[\int dr'\; f_L(r')\delta(r-r')\right] = f_L(r)\end{aligned}$$

Now we exploit that the radial functions ϕ_j do not depend on m_j and σ_j, so that we can average over m_j and σ_j. Note that here we assume that we average over complete angular momentm shells, which is not necessarily the case. Here caution is required.

$$g(\vec{r},\sigma) = -\sum_{L_g} Y_{L_g}(\vec{r})\delta_{\sigma,\sigma_f}\sum_{j=1}^{N}\sum_{\ell_\rho}\left(\frac{1}{2(2\ell_j+1)}\sum_{m_j}\sum_{m_\rho} C_{L_j,L_f,L_\rho}C_{L_j,L_g,L_\rho}\right)\phi_j^*(|\vec{r}|)v_{L_\rho}^{(j,f)}(|\vec{r}|)$$

The next step is only physically motivated and implies

$$\frac{4\pi}{(2\ell_1+1)(2\ell_2+1)}\sum_{m_1,m_2} C_{L_1,L_2,L_3}C_{L_1,L_2,L'_3} = K_{\ell_1,\ell_2,\ell_3}\delta_{L_3,L'_3}$$

$$\text{with} \qquad K_{\ell_1,\ell_2,\ell_3} = \frac{4\pi\sum_{m_1,m_2,m_3} C^2_{L_1,L_2,L_3}}{(2\ell_1+1)(2\ell_2+1)(2\ell_3+1)}$$

It has been tested empirically using the routine SPHERICAL$TESTGAUNTREL.

$$\begin{aligned}g(\vec{r},\sigma) &= -\sum_{L_g} Y_{L_g}(\vec{r})\delta_{\sigma,\sigma_f}\sum_{j=1}^{N}\sum_{\ell_\rho}\frac{2\ell_\rho+1}{8\pi}K_{\ell_j,\ell_\rho,\ell_f}\delta_{L_f,L_g}\phi_j^*(|\vec{r}|)v_{L_\rho}^{(j,f)}(|\vec{r}|) \\ &= \left[-\sum_{j=1}^{N}\sum_{\ell_\rho}\frac{2\ell_\rho+1}{8\pi}K_{\ell_j,\ell_\rho,\ell_f}\phi_j^*(|\vec{r}|)v_{L_\rho}^{(j,f)}(|\vec{r}|)\right]Y_{L_g}(\vec{r})\delta_{\sigma,\sigma_f} \\ &= \left[-\sum_{j=1}^{N}\sum_{\ell_\rho}\frac{2\ell_\rho+1}{8\pi}K_{\ell_j,\ell_\rho,\ell_f}\phi_j^*(|\vec{r}|)v_{L_\rho}^{(j,f)}(|\vec{r}|)\right]Y_{L_g}(\vec{r})\delta_{\sigma,\sigma_f}\end{aligned}$$

In the last step we exploited that the radial functions of $|\phi_j\rangle$ do not depend on the spin index. Because ths sum is always performed over complete shells including the spin multiplet, the δ-function has been replaced by a factor $\frac{1}{2}$. This step needs to be reconsidered when spin orbit coupling is introduced.

Thus we find, as expected from the rotational symmetry, that the potential preserves angular momentum and spin and that

$$g_{L_f,\sigma_f}(|\vec{r}|) = -\sum_{j=1}^{N}\sum_{\ell_\rho}\left(\frac{2\ell_\rho+1}{8\pi}K_{\ell_j,\ell_f,\ell_\rho}\right)\phi_j^*(|\vec{r}|)v_{L_\rho}^{(j,f)}(|\vec{r}|)$$

The recipe goes as follows

1. First we determine

$$K(\ell_j, \ell_\rho, \ell_f) \stackrel{\text{def}}{=} \frac{4\pi}{(2\ell_j+1)(2\ell_\rho+1)} \sum_{m_j, m_\rho} C^2_{L_j, L_\rho, L_f}$$

2. Then we determine

$$v_{L_\rho}(|\vec{r}|) = \int d^3r' \left[Y^*_{L_\rho}(\vec{r'} \frac{1}{|\vec{r'}|^2} \delta(|\vec{r}| - |\vec{r'}|) \right] \left[\int d^3r'' \frac{e^2}{4\pi\epsilon_0 |\vec{r} - \vec{r'}|} \phi_j(|\vec{r''}|) f(|\vec{r''}|) Y_{L_\rho}(\vec{r''}) \right]$$

   The routine radial$poisson solves

$$\begin{aligned}
v(\vec{r}) &= \int d^3r' \frac{e^2 \rho(\vec{r'})}{4\pi\epsilon_0 |\vec{r} - \vec{r'}|} \\
\rho(\vec{r}) &= \rho_L(|\vec{r}|) Y_L(\vec{r}) \\
v(\vec{r}) &= v_L(|\vec{r}|) Y_L(\vec{r}) \\
v_L(\vec{r}) &= \int d^3r'; \left[Y^*_L(\vec{r}) \frac{1}{|\vec{r'}^2} \delta(|\vec{r}| - |\vec{r'}|) \right] v(\vec{r}) \\
&= \int d^3r'; \left[Y^*_L(\vec{r}) \frac{1}{|\vec{r'}^2} \delta(|\vec{r}| - |\vec{r'}|) \right] \int d^3r'' \frac{e^2 \rho_L(|\vec{r''}|) Y_L(\vec{r''})}{4\pi\epsilon_0 |\vec{r'} - \vec{r''}|}
\end{aligned}$$

3. Finally we obtain the radial part of the result as

$$g_{L_f}(|\vec{r}|) = -\sum_j f_j \sum_{\ell_\rho} \frac{(2\ell_\rho + 1)}{8\pi} K_{\ell_j, \ell_\rho, \ell_f} \phi_j(|\vec{r}|) v_{L_\rho}(|\vec{r}|)$$

   In our notation the occupation f_j is unity, because the sum over j runs over all states. The occupation f_j has been introduced so that the sum over j can also be considered a sum over all shells.

Chapter 2

Setup construction and Setup parameters

2.1 Special cases

2.1.1 Oxygen molecule

The oxygen molecule is one of the most challenging systems. The reason is the following.

- It is a small atom because it is on the very right of the periodic table. The large effective core charge results in a small atomic radius. Furthermore it has many electrons that contribute to the total energy. Finally, compared to the atoms such as fluorine and neon it forms strong bonds.
- the bond distance is very short. It amounts to only 83 % of the sum of the covalent radii.

For this reason, oxygen is probably the single one atom that determines the plane wave cutoff that needs to be used for general materials. It is therefore important to determine the cutoff radii for the pseudization carefully. In Fig. 2.1 we show the atomization energy as function of cutoff radius.

The total energy is not completely converged wuth a plane wave cutoff of 60 Ry for the density.

```
!SPECIES   NAME='O_'  M=80. NPRO=1 1 1 LRHOX=4 RAD/RCOV=1.4
  !NTBO    NOFL=1 1 0 CV=T LHFWEIGHT=0.100
           TAILLAMBDA=4.0 2.0 RAUG/RCOV=1.2 RTAIL/RCOV=1.4
  !END
  !AUGMENT ID='MY_NDLSS_O' EL='O' ZV= 6.
           TYPE='NDLSS' RBOX/RCOV=1.2 RCSM/RCOV=.25
           RCL/RCOV=.65 0.65 0.65 0.65
    !GRID  DMIN=1.E-6 DMAX=.15 RMAX=9. !END
    !POT   POW=3. RC/RCOV=0.65 VAL0_X=-3.8 !END
    !CORE  POW=2. RC/RCOV=.65 !END
  !END
!END
```

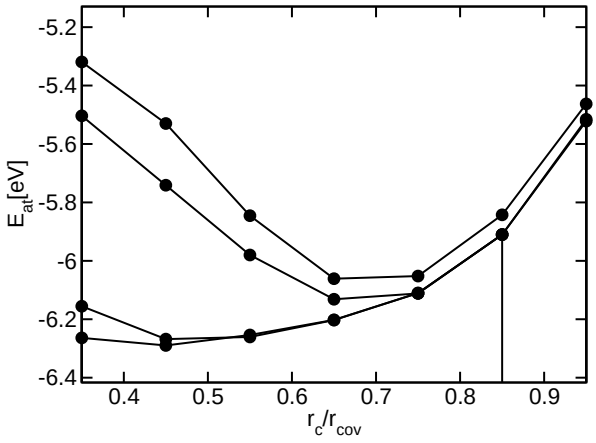

Fig. 2.1: The atomization energy of the oxygen molecule as function of the cutoff radius (in units of the covalent radius) for the partial wave pseudization. The calculations have been computed with plane wave cutoffs of 30 Ry, 50 Ry, 100 Ry and 150 Ry. The plane wave cutoff for the density was twice that for the wave functions. The pseudization has been performed with the nodeless construction. The calculation has been done with the PBE functional. The data with $E_{PW} = 30$ Ry are shifted because the plane wave cutoff for the density is too low.

2.1.2 Hydrogen

Hydrogen is the second most important element, because it often saturates bonds. Therefore, I explore the hydrtogen molecule and water as its oxide.

Important Remark! Special caution is required because the h-atom nearly impossible to calculate with full spin poslarization: The density of one spin direction vanishes completely. Therfore the hydrogen atom is calculated with a moment of 0.499 $\hbar$. An energy of 2.544 mH needs to be subtracted from the calculated energy of the isolated atom.

As seen in Fig. 2.2, the reaction energy from the hydrogen molecule and the water molecule is nearly independent of the cutoff radius up to the covalent radius. The atomization energy, however, depends strongly on the cutoff: It changes by about 0.05 eV from $r_c = 0.5 r_{cov}$ to $r_c = 1.0 r_{cov}$. While we cannot say which is the optimum result we will use $r_c = 1.2\ r_{cov}$. Up to this radius the reaction energy H_2+O→H_2O is still independent of the radius, and the atomization energy of the hydrogen molecule becomes independent of the radius for larher distances. (This is only a weak argument, though.) Finally we consider the plane wave convergence to choose the larger radius. While hydrogen does not dominate convergence as individual atom, there are usually many hydrogen atoms in a material.

```
!SPECIES   NAME='H_'  M=2. NPRO=1 1 LRHOX=2 RAD/RCOV=1.2
  !NTBO    NOFL=1 0 CV=T LHFWEIGHT=0.100
           TAILLAMBDA=4.0 2.0 RAUG/RCOV=1.2 RTAIL/RCOV=1.4
  !END
  !AUGMENT ID='MY_NDLSS_H' EL='H' ZV= 1.
           TYPE='NDLSS' RBOX/RCOV=1.2 RCSM/RCOV=.25
           RCL/RCOV=1.2 1.2  1.2  1.2
    !GRID  DMIN=1.E-6 DMAX=.15 RMAX=9. !END
```

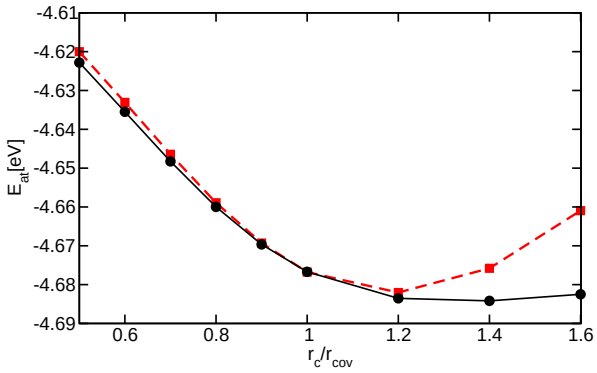

Fig. 2.2: The atomization energy of the hydrogen molecule (black, circles) as function of the cutoff radius (in units of the covalent radius) for the partial wave pseudization. The calculations have been computed with a plane wave cutoff of 50 Ry. The plane wave cutoff for the density was twice that for the wave functions. The pseudization has been performed with the nodeless construction. The calculation has been done with the PBE functional.

```
    !POT   POW=3. RC/RCOV=1. VALO_X=-1.6 !END
    !CORE  POW=2. RC/RCOV=1.  !END
  !END
!END
```

2.1.3 Carbon

Due to its importance in organic chemistry and biochemistry, carbon is considered the third most important element.

Interesting is that the energies shown in Fig. 2.3 are fairly independent of the chosen pseudization cutoff if the plane wave cutoff is sufficiently large. This is probably due to the nodeless construction, for which the pseudo wave function turns continuously into the nodeless wave function when the radius is reduced, which the traditional construction introduces a node or a sharp turn to avoid the node.

This behavior (independce of the energy from the pseudization radius) is very different from that for oxygen, for which the energy of the oxygen molecule depends strongly on the pseudization radius. In Fig. 2.3 we studied also CO and CO2. Here the behavior is close to that of the oxygen molecule.

```
!SPECIES   NAME='C_'  M=40. NPRO=1 1 1 LRHOX=4 RAD/RCOV=1.4
  !NTBO    NOFL=1 1 0 CV=T LHFWEIGHT=0.100
           TAILLAMBDA=4.0 2.0 RAUG/RCOV=1.2 RTAIL/RCOV=1.4
  !END
  !AUGMENT ID='MY_NDLSS_C' EL='C' ZV= 4.
           TYPE='NDLSS' RBOX/RCOV=1.2 RCSM/RCOV=.25
           RCL/RCOV=0.85 0.85 0.85 0.85
    !GRID  DMIN=1.E-6 DMAX=.15 RMAX=9. !END
    !POT   POW=3. RC/RCOV=0.75  VALO_X=-2.7 !END
```

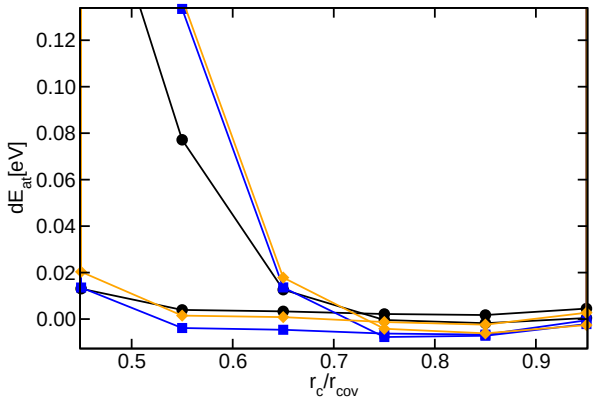

Fig. 2.3: The atomization energy of the methane CH_4 (black circle), Ethene C_2H_4 (blue square) and ethane C_2H_6 (orange diamond) as function of the pseudization cutoff radius (in units of the covalent radius) for carbon. The calculations have been computed with a plane wave cutoff of 50 Ry and 100 Ry. The plane wave cutoff for the density was twice that for the wave functions. The pseudization has been performed with the nodeless construction. The calculation has been done with the PBE functional.

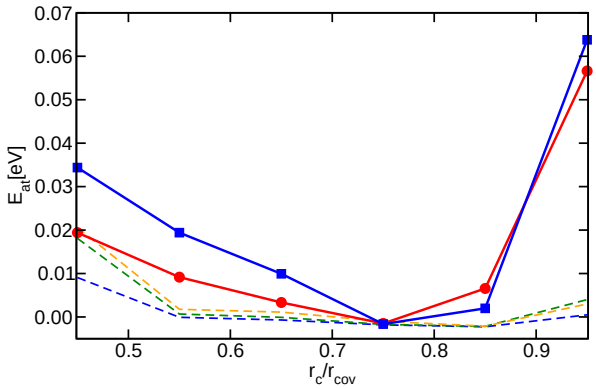

Fig. 2.4: The atomization energy of CO (red circle) and CO_2 blue square) as function of the pseudization radius (in units of the covalent radius) for carbon. Also shown are the total energies of methane CH_4 (blue dashed), Ethene C_2H_4 (green dashed) and ethane C_2H_6 (orange dashed). The calculations have been computed with a plane wave cutoff of 100 Ry. The plane wave cutoff for the density is twice that for the wave functions. The pseudization has been performed with the nodeless construction. The calculation has been done with the PBE functional.

```
      !CORE  POW=2. RC/RCOV=0.75  !END
    !END
  !END
```

2.1.4 Setups for the G2 database

```
!SPECIES   NAME='H_'  M=2. NPRO=1 1 LRHOX=2 RAD/RCOV=1.2
```

```
  !NTBO    NOFL=1 0 CV=T LHFWEIGHT=0.100
           TAILLAMBDA=4.0 2.0 RAUG/RCOV=1.2 RTAIL/RCOV=1.4
  !END
  !AUGMENT ID='MY_NDLSS_H' EL='H' ZV= 1.
           TYPE='NDLSS' RBOX/RCOV=1.2 RCSM/RCOV=.25
           RCL/RCOV=1.2 1.2  1.2  1.2
    !GRID  DMIN=1.E-6 DMAX=.15 RMAX=9. !END
    !POT   POW=3. RC/RCOV=1.2 VAL0_X=-1.6 !END
    !CORE  POW=2. RC/RCOV=1.2 !END
  !END
!END

!SPECIES   NAME='LI'  M=40. NPRO=1 1  LRHOX=4 RAD/RCOV=1.0
  !NTBO    NOFL=1 0 0 CV=T LHFWEIGHT=0.100
           TAILLAMBDA=4.0 2.0 RAUG/RCOV=1.2 RTAIL/RCOV=1.4
  !END
  !AUGMENT ID='MY_NDLSS_LI' EL='LI' ZV= 1.
           TYPE='NDLSS' RBOX/RCOV=1.2 RCSM/RCOV=.25
           RCL/RCOV=.861 .861 .861  .861
    !GRID  DMIN=1.E-6 DMAX=.15 RMAX=9. !END
    !POT   POW=3. RC/RCOV=.861 VAL0_X=-0.8 !END
    !CORE  POW=2. RC/RCOV=.861  !END
  !END
!END

!SPECIES   NAME='BE'  M=40. NPRO=1 1 0 LRHOX=2 RAD/RCOV=1.4
  !NTBO    NOFL=1 1 0 CV=T LHFWEIGHT=0.100
           TAILLAMBDA=4.0 2.0 RAUG/RCOV=1.2 RTAIL/RCOV=1.4
  !END
  !AUGMENT ID='MY_NDLSS_BE' EL='BE' ZV= 2.
           TYPE='NDLSS' RBOX/RCOV=1.2 RCSM/RCOV=.25
           RCL/RCOV=.882 .882 .882 .882
    !GRID  DMIN=1.E-6 DMAX=.15 RMAX=9. !END
    !POT   POW=3. RC/RCOV=.882 VAL0_X= -1.6 !END
    !CORE  POW=2. RC/RCOV=.882 !END
  !END
!END

!SPECIES   NAME='B_'  M=40. NPRO=1 1 1 LRHOX=4 RAD/RCOV=1.4
  !NTBO    NOFL=1 1 0 CV=T LHFWEIGHT=0.100
           TAILLAMBDA=4.0 2.0 RAUG/RCOV=1.2 RTAIL/RCOV=1.4
  !END
  !AUGMENT ID='MY_NDLSS_B' EL='B' ZV= 3.
           TYPE='NDLSS' RBOX/RCOV=1.2 RCSM/RCOV=.25
           RCL/RCOV=.75 .75 .75 .75
    !GRID  DMIN=1.E-6 DMAX=.15 RMAX=9. !END
    !POT   POW=3. RC/RCOV=.774 VAL0_X= -3.9 !END
```

```
    !CORE  POW=2. RC/RCOV=.774 !END
  !END
!END

!SPECIES   NAME='C_'  M=40. NPRO=1 1 1 LRHOX=4 RAD/RCOV=1.4
  !NTBO    NOFL=1 1 0 CV=T LHFWEIGHT=0.100
           TAILLAMBDA=4.0 2.0 RAUG/RCOV=1.2 RTAIL/RCOV=1.4
  !END
  !AUGMENT ID='MY_NDLSS_C' EL='C' ZV= 4.
           TYPE='NDLSS' RBOX/RCOV=1.2 RCSM/RCOV=.25
           RCL/RCOV=0.85 0.85 0.85 0.85
    !GRID  DMIN=1.E-6 DMAX=.15 RMAX=9. !END
    !POT   POW=3. RC/RCOV=0.75  VAL0_X=-2.7 !END
    !CORE  POW=2. RC/RCOV=0.75  !END
  !END
!END

!SPECIES   NAME='N_'  M=40. NPRO=1 1 1 LRHOX=4 RAD/RCOV=1.4
  !NTBO    NOFL=1 1 0 CV=T LHFWEIGHT=0.100
           TAILLAMBDA=4.0 2.0 RAUG/RCOV=1.2 RTAIL/RCOV=1.4
  !END
  !AUGMENT ID='MY_NDLSS_N' EL='N' ZV= 5.
           TYPE='NDLSS' RBOX/RCOV=1.2 RCSM/RCOV=.25
           RCL/RCOV=0.75 0.75 0.75  0.75
    !GRID  DMIN=1.E-6 DMAX=.15 RMAX=9. !END
    !POT   POW=3. RC/RCOV=0.75 VAL0_X=-4.3 !END
    !CORE  POW=2. RC/RCOV=0.75  !END
  !END
!END

!SPECIES   NAME='O_'  M=80. NPRO=1 1 1 LRHOX=4 RAD/RCOV=1.4
  !NTBO    NOFL=1 1 0 CV=T LHFWEIGHT=0.100
           TAILLAMBDA=4.0 2.0 RAUG/RCOV=1.2 RTAIL/RCOV=1.4
  !END
  !AUGMENT ID='MY_NDLSS_O' EL='O' ZV= 6.
           TYPE='NDLSS' RBOX/RCOV=1.2 RCSM/RCOV=.25
           RCL/RCOV=.65 0.65 0.65 0.65
    !GRID  DMIN=1.E-6 DMAX=.15 RMAX=9. !END
    !POT   POW=3. RC/RCOV=0.65 VAL0_X=-3.8 !END
    !CORE  POW=2. RC/RCOV=.65 !END
  !END
!END

!SPECIES   NAME='F_'  M=80. NPRO=1 1 1 LRHOX=2 RAD/RCOV=1.4
  !NTBO    NOFL=1 1 0 CV=T LHFWEIGHT=0.100
           TAILLAMBDA=4.0 2.0 RAUG/RCOV=1.2 RTAIL/RCOV=1.4
  !END
```

```
  !AUGMENT ID='MY_NDLSS_F' EL='F_' ZV= 7.
           TYPE='NDLSS' RBOX/RCOV=1.2 RCSM/RCOV=.25
           RCL/RCOV=0.8 0.8 0.8  0.8
    !GRID  DMIN=1.E-6 DMAX=.15 RMAX=9. !END
    !POT   POW=3. RC/RCOV=0.75 VAL0_X=-3.5 !END
    !CORE  POW=2. RC/RCOV=0.75  !END
  !END
!END

!SPECIES   NAME='Na'  M=40. NPRO=2 2 1 LRHOX=4 RAD/RCOV=1.0
  !NTBO    NOFL=1 1 0 CV=T LHFWEIGHT=0.100
           TAILLAMBDA=4.0 2.0 RAUG/RCOV=1.2 RTAIL/RCOV=1.4
  !END
  !AUGMENT ID='MY_NDLSS_NA' EL='NA' ZV= 9.
           TYPE='NDLSS' RBOX/RCOV=1.2 RCSM/RCOV=.25
           RCL/RCOV=0.780 0.790 0.804
    !GRID  DMIN=1.E-6 DMAX=.15 RMAX=9. !END
    !POT   POW=3. RC/RCOV=0.766 VAL0_X=-1.1  !END
    !CORE  POW=2. RC/RCOV=0.766  !END
  !END
!END

!SPECIES   NAME='Al'  M=40. NPRO=2 2 1 LRHOX=4 RAD/RCOV=1.0
  !NTBO    NOFL=1 1 0 CV=T LHFWEIGHT=0.100
           TAILLAMBDA=4.0 2.0 RAUG/RCOV=1.2 RTAIL/RCOV=1.4
  !END
  !AUGMENT ID='MY_NDLSS_AL' EL='AL' ZV= 3.
           TYPE='NDLSS' RBOX/RCOV=1.2 RCSM/RCOV=.25
           RCL/RCOV=.919 .919 .919 .919
    !GRID  DMIN=1.E-6 DMAX=.15 RMAX=9. !END
    !POT   POW=3. RC/RCOV=.919 VAL0_X= -1.5 !END
    !CORE  POW=2. RC/RCOV=.919 !END
  !END
!END

!SPECIES   NAME='Si'  M=40. NPRO=2 2 1 LRHOX=4 RAD/RCOV=1.4
  !NTBO    NOFL=1 1 0 CV=T LHFWEIGHT=0.100
           TAILLAMBDA=4.0 2.0 RAUG/RCOV=1.2 RTAIL/RCOV=1.4
  !END
  !AUGMENT ID='MY_NDLSS_SI' EL='SI' ZV= 4.
           TYPE='NDLSS' RBOX/RCOV=1.2 RCSM/RCOV=.25
           RCL/RCOV=0.953 0.953 0.953 0.953
    !GRID  DMIN=1.E-6 DMAX=.15 RMAX=9. !END
    !POT   POW=3. RC/RCOV=0.953  VAL0_X= -1.8 !END
    !CORE  POW=2. RC/RCOV=0.953  !END
  !END
!END
```

```
!SPECIES   NAME='P_'  M=40. NPRO=2 2 1 LRHOX=2 RAD/RCOV=1.4
  !NTBO    NOFL=1 1 0 CV=T LHFWEIGHT=0.100
           TAILLAMBDA=4.0 2.0 RAUG/RCOV=1.2 RTAIL/RCOV=1.4
  !END
  !AUGMENT ID='MY_NDLSS_P' EL='P_' ZV= 5.
           TYPE='NDLSS' RBOX/RCOV=1.2 RCSM/RCOV=.25
           RCL/RCOV=0.899 0.899 0.899  0.899
    !GRID  DMIN=1.E-6 DMAX=.15 RMAX=9. !END
    !POT   POW=3. RC/RCOV=.899 VAL0_X=-2.4 !END
    !CORE  POW=2. RC/RCOV=.899 !END
  !END
!END

!SPECIES   NAME='S_'  M=40. NPRO=2 2 1 LRHOX=4 RAD/RCOV=1.4
  !NTBO    NOFL=1 1 0 CV=T LHFWEIGHT=0.100
           TAILLAMBDA=4.0 2.0 RAUG/RCOV=1.2 RTAIL/RCOV=1.4
  !END
  !AUGMENT ID='MY_NDLSS_S' EL='S_' ZV= 6.
           TYPE='NDLSS' RBOX/RCOV=1.2 RCSM/RCOV=.25
           RCL/RCOV=0.954 0.960  0.882  0.882
    !GRID  DMIN=1.E-6 DMAX=.15 RMAX=9. !END
    !POT   POW=3. RC/RCOV=0.742 VAL0_X=-3.3 !END
    !CORE  POW=2. RC/RCOV=0.742 !END
  !END
!END

!SPECIES   NAME='CL'  M=40. NPRO=2 2 1 LRHOX=2 RAD/RCOV=1.4
  !NTBO    NOFL=1 1 0 CV=T LHFWEIGHT=0.100
           TAILLAMBDA=4.0 2.0 RAUG/RCOV=1.2 RTAIL/RCOV=1.4
  !END
  !AUGMENT ID='MY_NDLSS_CL' EL='CL' ZV= 7.
           TYPE='NDLSS' RBOX/RCOV=1.2 RCSM/RCOV=.25
           RCL/RCOV=0.802 0.802 0.802 0.802
    !GRID  DMIN=1.E-6 DMAX=.15 RMAX=9. !END
    !POT   POW=3. RC/RCOV=0.802 VAL0_X=-3.5 !END
    !CORE  POW=2. RC/RCOV=0.802  !END
  !END
!END

!SPECIES   NAME='Br'  M=40. NPRO=1 1 1 LRHOX=2 RAD/RCOV=1.4
  !NTBO    NOFL=1 1 0 CV=T LHFWEIGHT=0.100
           TAILLAMBDA=4.0 2.0 RAUG/RCOV=1.2 RTAIL/RCOV=1.4
  !END
  !AUGMENT ID='MY_NDLSS_BR' EL='BR' ZV= 7.
           TYPE='NDLSS' RBOX/RCOV=1.2 RCSM/RCOV=.25
           RCL/RCOV=.975 .975 .975 .975
```

```
    !GRID  DMIN=1.E-6 DMAX=.15 RMAX=9. !END
    !POT   POW=3. RC/RCOV=.975 VALO_X= -2.0 !END
    !CORE  POW=2. RC/RCOV=.975 !END
  !END
!END
```

Results

The results are shown in Fig. 2.5. The large deviation between CP-PAW and Scuseria's result may be due to the fact that these are the largest molecules. (On my side I need to optimize the atomic structure with the new setups.)

The largest deviations from Vasp and GPAW are for

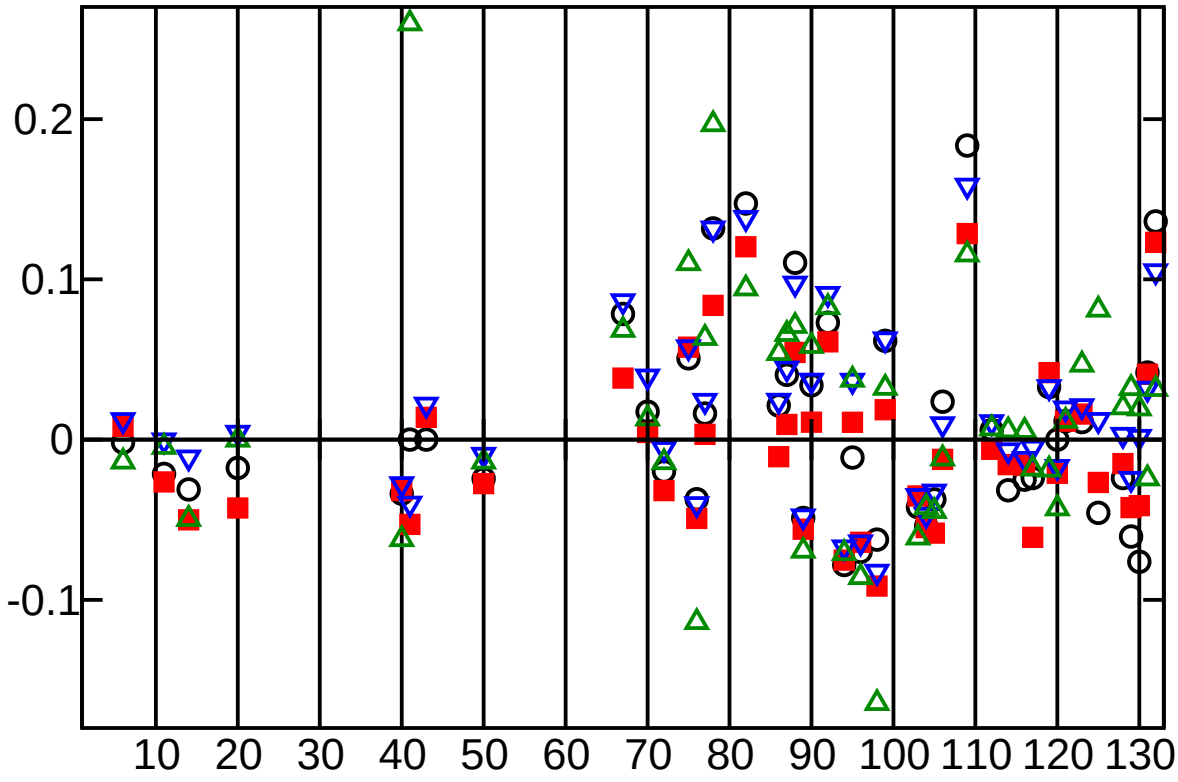

Fig. 2.5: Deviation from the CP-PAW result for the atomization energy in eV in the G2 database for GPAW (black), VASP (red), Gauss (blue), Scuseria (green). The molecules are identified in alphabetical order (Careful! not unique!).

2.1.5 Transition metals

The biggest challenge for transition metal atoms are the p-states. They have a maximum that lies very far out. If one pseudizes this wave function a sharp bend is required to avoid introduing nodes.

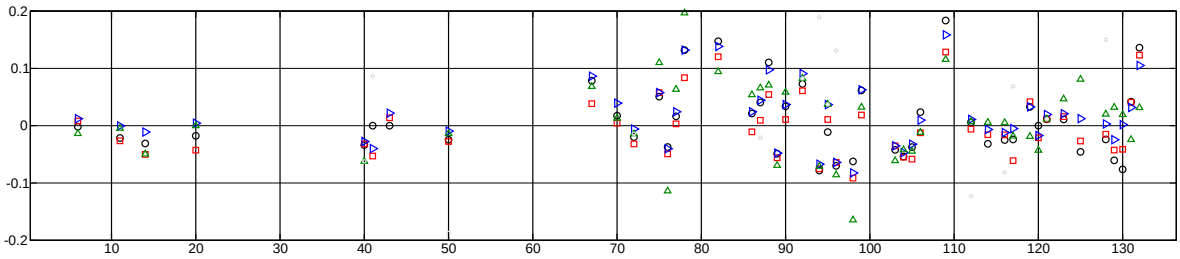

Fig. 2.6: Deviation from the CP-PAW result for the atomization energy in eV in the G2 database for GPAW (black), VASP (red), Gauss (blue), Scuseria (green). The molecules are identified in alphabetical order (Careful! not unique!).

- The best remedy is to include the semi-core states with the same quantum number as the d-electrons. They have a similar radial extent. The valence s and p-states will have nodes in a natural way.
- Restricting the valence electrons to teh true valence states requires that the pseudization radius for the s and p states is moved sufficiently far out, so that a reasonable shape of the pseudo partial waves results.

2.1.6 Benchmarks

- 2005 Paier[7]:

	Kresse
H	0.8
Li	1.3
Be	1.9
C	1.1
N	1.1
O	1.1
F	1.0
Si	1.9
P	1.5
S	1.5
Cl	1.5
Na	1.7

The data “Kresse” are the cutoff parameters for the pseudo wave functions in VASP according to Paier[7].

Chapter 3

Code structure

3.1 Code to construct automatic stp.cntl file

The routines SETUP_BUILDPARMS_NDLSS constructs an automatic parameter file stp.cntl for the atomic setups. There are alternatives called SETUP_BUILDPARMS_1 for the standard setups and SETUP_BUILDPARMS_2 for the HBS-type setups.

```
!SETUP  ID='H_NDLSS' EL='H' ZV= 1.
        TYPE='NDLSS' RBOX/RCOV=2. RCSM/RCOV=0.25
        RCL/RCOV= 1.0 1.0 1.0 1.0 1.
        LAMBDA= 6. 6. 6. 6. 6.
  !GRID DMIN=1.E-6 DMAX=0.1 RMAX= 9. !END
  !POT  POW=3.  RC/RCOV=0.67 !END
  !CORE POW=3.  RC/RCOV=0.67 !END
!END
```

- ZV: For main group elements, the d-electron and f-electron shells are not considered part of the valence shell.
- RBOX/RCOV=2.
- RCSM/RCOV=0.25
- RCL/RCOV=0.75
- RCL/RCOV=6.
- GRID: DMIN=5×10^{-6}, DMAX=5×10^{-1}, RMAX is $2r_{cov}$ or $r_{cov} + 0.73$ Å/a_0, whatever is larger
- POT:

3.2 Flowchart of the paw_setups object

This is lifted from my notes and needs to be updated.

1. collect input data

   - AEZ: atomic number
   - ZV: Number of valence electros
   - $r_{c,\ell}$,λ_ℓ: Parameters for pseudo-partial-wave construction
   - $r_{c,small}$: The compensation density is proportional to $e^{-(r/r_{c,small})^2}$
   - $r_{c,big} = 1/\sqrt{0.218}$. The extended compensation density is proportional to $e^{-(r/r_{c,big})^2}$ (currently hardwired, probably too small.)
   - $\lambda, r_c, f(r=0)$: Parameters for pseudopotential construction
   - $\lambda, r_c, f(r=0)$: Parameters for pseudocore construction
   - The radial grid is encoded in grid-id "GID"
   - Atomic mass
   - PSG2,PSG4
   - NPRO number of partial waves per l-channel
   - LRHOX density is expanded up to maximum angular momentum LRHOX

2. AESCF performs an all-electron self-consistent DFT calculation: The boundary condition is a hard box with radius equal to the third-last radial grid point. The calculation considers only spherical densities and ignores spin-polarization. This is important so that the setup construction does not artificially break the symmetry of the environment.

   One obtains the potential $v(\vec{r})$ of the all-electron atom, the all-electron wave functions $|\psi_n\rangle$., the one-particle energies ϵ_n

   The procedure is described in more detail in section 3.3.

3. ISCATT is a variable that is zero for the occupied partial wave with the highest energy for a given angular momentum. ISCATT=-1 identifies a semi-core state, and ISCATT=1 identifies a scattering state.

4. calculate all-electron core density $n^C(\vec{r})$.

5. calculate pseudo core density pscore $\tilde{n}^C(\vec{r})$ from the all-electron core density. The method is described in section 1.3.

6. MAKEPARTIALWAVES

   - **pseudo potential:** construct pseudopotential PSPOT from the all-electron potential in a hard box with radius ROUT, provided on input. The method is described in section 1.3.
   - **nodeless atomic wave functions:** construct nodeless wave functions UOFI. Even for calculations with a Fock contribution, UOFI will be determined here only for the local potential and it will be updated later with the Fock potential.

$$\left[\hat{h}_{loc} - \epsilon_n\right] |u_n\rangle = |u_{n-1}\rangle$$
$$u_n(0) = \partial_r u_n(0) = 0 \qquad \text{for} \qquad n > 0$$

- **nodeless partial waves:** construct nodeless partial waves NLPHI. The lowest partial wave for each ℓ will be constructed with a hard sphere potential at radius ROUT, just as the nodeless wave function constructed above. The higher partial waves will be constructed with the same logarithmic derivative at RBND as the first partial wave for the same ℓ.

  The lowest partial wave for each ℓ uses the highest core state as inhomogneity, while the higher partial waves use the next lower partial wave as inhomogeneity. Thus a sequence of nodeless partial waves in introduced. One potential disadvantage of this construction is that the inhomogeneity extends further out with each partial wave.

$$\begin{aligned}\left[\hat{h}_{loc}-\bar{\epsilon}_n\right]|\phi_n^{nl}\rangle &= |\phi_{n-1}^{nl}\rangle \\ \hat{t}|\phi_n^{nl}\rangle &= |\phi_{n-1}^{nl}\rangle + (\bar{\epsilon}_n - v)|\phi_n^{nl}\rangle\end{aligned}$$

  where $|\phi_{-1}^{nl}\rangle = |u_c\rangle$ is the nodeless wave function of the highest core state. The energies $\bar{\epsilon}_n$ for the partial waves are EOFLN. (The energies of the atomic wave functions are EOFI).

  (Using the parameter TSMALLBOX=T the boundary conditions can be changed so that all partial waves experience a hard sphere at RBND. This choice has the disadvantage that the lowest partial wave is chosen at a fairly high energy.)

- **add Fock term to nodeless wave functions:** This step is only done for Fock contribution in the potential: Starting from the nodeless wave function obtained for the local potential only, the nodeless atomic wave functions are constructed with the Fock contribution.

$$\begin{aligned}\left(\hat{h}_{loc}-\epsilon_0\right)|\phi'\rangle &= -\left(\hat{h}_{loc}+v_{nl}-\epsilon_0\right)|\phi_0\rangle + |g\rangle \\ \left(\hat{h}_{loc}-\epsilon'\right)|\dot{\phi}\rangle &= |\phi_0\rangle \\ \left(\hat{h}_{loc}-\epsilon'\right)|\phi_{hom}\rangle &= 0 \\ |\phi\rangle &= |\phi_0\rangle + |\phi'\rangle + |\dot{\phi}\rangle\delta\epsilon + |\phi_{hom}\rangle\alpha\end{aligned}$$

  The variables are adjusted to fulfill the boundary conditions. The inhomogeneity is adapted as well. The basic equation is derived later in Section 1.5.1.

- **add Fock term to partial waves:** This step is only done for Fock contribution in the potential: Starting from the nodeless partial waves and the inhomogeneity constructed consistently with the Fock potential the nodeless partial waves are updated.

- **rescale:** rescale wave functions and partial waves such that the first partial wave is normalized. Only one scale factor per ℓ is allowed!

- For plotting purposes, we introduce factors f_n^{ϕ} =PHISCALE for the partial waves and f_n^{ψ} =PSISCALE for the energy eigenstates, so that $|u_n\rangle f_n$. have about the same size.

$$f_n^{\psi} = \prod_{j=1}^{n}(\epsilon_j - \epsilon_n)$$

$$f_{\alpha}^{\phi} = \prod_{j=c+1}^{\alpha}(\bar{\epsilon}_j - \bar{\epsilon}_{\alpha})$$

  where the sum includs only states with the same angular momentum.

- **node-reduced partial waves:** construct $|q_{c+1}(\epsilon_n)\rangle$ functions, named `QN`. Here c is the index of the highest state treated explicitely as core state. Thus the index $c+1$ refers to the first wave function included in the valence shell. The functions $|q_{c+1}(\epsilon_{n+i})\rangle$ are not necessarily nodeless. The number of nodes for the $|q_{c+1}(\epsilon)\rangle$ function is equal to the number of nodes of the corresponding all-electron partial wave $|\phi(\epsilon)\rangle$ minus the number of core states with the same angular momentum.

  We use Eq. **??** which is repeated below:

$$|q_{c+1}(\epsilon_n)\rangle \stackrel{\text{Eq. ??}}{=} \sum_{i=c+1}^{n} |\phi_i^{nl}\rangle \prod_{j=c+1}^{i-1} (\bar{\epsilon}_n - \bar{\epsilon}_j)$$

  This implies that the $|q_{c+1}(\epsilon_n)\rangle$ and $|\phi_n^{nl}\rangle$ functions are scaled such that their long-range tails differ. The long range parts behave as

$$|q_{c+1}(\epsilon_n)\rangle \leftrightarrow |\phi_n^{nl}\rangle \prod_{j=c+1}^{n-1} (\epsilon_n - \epsilon_j)$$

  Thus we introduce a factor $qby u_n = \prod_{j=c+1}^{n-1} \frac{1}{\bar{\epsilon}_n - \bar{\epsilon}_j}$.

  A matrix $\boldsymbol{T}$ is constructed that describes the transformation from the nodeless partial waves to the $|q_{c+1}(\epsilon_n)\rangle$ functions.

$$|q_{c+1}(\epsilon_n)\rangle = \sum_m |\phi_m^{nl}\rangle T_{m,n}$$

  This matrix will later allow to perform the back transform.

- **rescale nodeless partial waves:** The nodeless $|\phi_n^{nl}\rangle$ functions are now rescaled so that that their long-range-behavior matches that of $|q_{c+1}(\epsilon_{n+i})\rangle$. The scale factor is `ubyq`$= 1/T_{n,n}$, i.e. $|\phi_n^{nl}\rangle \leftarrow |\phi_n^{nl}\rangle T_{n,n}$.

  The scaling of $|q_{c+1}(\epsilon_n)\rangle$ has been adopted because the pseudization has to depend on the q-function. Pseudization to nodeless functions does not work over several bands.

  From now on we **must no more use** the relation $(\hat{h} - \epsilon_n)|\phi_n^{nl}\rangle = |\phi_{n-1}^{nl}\rangle$!

- **all-electron partial waves:** Construct all-electron partial waves by mixing in the core states. We use the nodeless construction instead of reorthogonalization. (The two methods differ because the small component is ignored.)

  We use Eq. 3.1 which has the form

$$|\phi(\epsilon_n)\rangle = |q_{c+1}(\epsilon_n)\rangle + \sum_{i=1}^{c} |u_i\rangle \prod_{j=i}^{c} \frac{1}{\bar{\epsilon}_n - \epsilon_j}$$

- **pseudo partial waves:** Construct pseudo partial waves
  - Type HBS: The technique is analogous to the procedure of Hamann Bachelet Schlüter. The equation

$$\left[\frac{\vec{p}^2}{2m} + \tilde{v} + A\mathrm{e}^{-\left(\frac{r}{r_{c,\alpha}}\right)^{\lambda_\alpha}} - \epsilon_\alpha\right] |\tilde{\phi}_\alpha\rangle = 0$$

is solved iteratively with differing A until the logaritmic derivative and the number of nodes of the pseudo and true partial wave are identical. The logarithmic derivative is taken at a radius beyond which the following two conditions are fulfilled

$$\left|\frac{1}{\langle\vec{r}|q_n(\epsilon_\alpha)\rangle}\langle\vec{r}|\frac{p^2}{2m}+\tilde{v}-\epsilon_\alpha|q_n(\epsilon_\alpha)\rangle\right| < 10^{-5}$$
$$e^{-\left(\frac{r}{r_{c,\alpha}}\right)^{\lambda_\alpha}} < 10^{-8}$$

Note that this does not require the all-electron and the pseudo potential or partial waves to be identical! The partial waves may differ by an admixture of the core wave functions.
Number of nodes and logarithmic derivative are encoded in the function

$$\alpha(\epsilon) \stackrel{\text{def}}{=} \frac{1}{2}-\frac{1}{\pi}\text{atan}(\frac{\partial_r\phi(\epsilon,r)}{\phi(\epsilon,r)})+NN$$

which I will name generalized phaseshift. According to the Wigner rule, a band would lie between an half-integer and an integer value of this generalized phaseshift.

$$\partial_r\phi=0 \quad \Rightarrow \quad \alpha=NN+\frac{1}{2} \quad \text{bond}$$
$$\phi=0 \quad \Rightarrow \quad \alpha=NN+1 \quad \text{antibond}$$

  - Type Kerker:

- construct bare projectors $\langle\bar{p}_\alpha|$:

$$|\bar{p}_\alpha\rangle=\left[\frac{\vec{p}^2}{2m}+\tilde{v}-\epsilon_\alpha\right]|\tilde{\phi}_\alpha\rangle$$

This is a result of the closure relation that the PAW equations are exactly fulfilled for the pseudo partial waves.

- Biorthogonality $\langle\tilde{p}_\alpha|\tilde{\phi}_\beta\rangle=\delta_{\alpha,\beta}$:
The biorthogonality is enforced by a Gram-Schmidt-like procedure

$$|\tilde{\phi}'_\alpha\rangle=\sum_\beta|\tilde{\phi}_\beta\rangle A_{\beta\alpha}$$
$$|\tilde{p}'_\alpha\rangle=\sum_\beta|\bar{p}_\beta\rangle B_{\beta,\alpha}$$

so that

$$\langle\tilde{p'}_\alpha|\tilde{\phi}'_\beta\rangle=\delta_{\alpha,\beta}$$

The matrices $\boldsymbol{A}$ and $\boldsymbol{B}$ are triangular, i.e. $A_{i,j}=0$ for $i>j$ and similar for $\boldsymbol{B}$.
So-far, only the matrices $\boldsymbol{A}$ and $\boldsymbol{B}$ have been computed. The partial waves and projector functions are not updated. Once the matrices A and B have been computed we cal

$$|\tilde{\phi}^{new}_\alpha\rangle=|\tilde{\phi}_\alpha\rangle$$
$$|\tilde{p}^{new}_\alpha\rangle=\sum_\beta|\bar{p}_\beta\rangle C_{\beta,\alpha} \qquad \text{with } \boldsymbol{C}=\boldsymbol{B}\boldsymbol{A}^\dagger$$

Only the projector functions are transformed. The partial waves remain unchanged and keep their physical meaning.

- Determine

$$
\begin{aligned}
dT_{\alpha,\beta} &= \langle\phi_\alpha|\frac{\vec{p}^2}{2m}|\phi_\beta\rangle - \langle\tilde{\phi}_\alpha|\frac{\vec{p}^2}{2m}|\tilde{\phi}_\beta\rangle \\
dO_{\alpha,\beta} &= \langle\phi_\alpha|\phi_\beta\rangle - \langle\tilde{\phi}_\alpha|\tilde{\phi}_\beta\rangle \\
dH_{\alpha,\beta} &= \langle\phi_\alpha|\frac{\vec{p}^2}{2m} + v|\phi_\beta\rangle - \langle\tilde{\phi}_\alpha|\frac{\vec{p}^2}{2m} + \tilde{v}|\tilde{\phi}_\beta\rangle
\end{aligned}
$$

In practive we do not use the kinetic energy operator $\hat{t} = \frac{\hat{\vec{p}}^2}{2m}$, but the expression $\hat{t}|\phi_\alpha\rangle = (\epsilon_\alpha - v)|\phi_\alpha\rangle$. There are two reasons for it. Applying a differential operator to a function stored on a grid, introduces numerical noise. The differential operator as used by us is strictly consistent with the Schrödinger equation including all numeric errors. Last but not least, our method automatically incorporates relativistic effects in the PAW method.

- construct scattering wave functions:

  First the nodeless scattering wave function is constructed

$$(\hat{h} - \epsilon_\gamma)|u^{scatt}\rangle = |u_n\rangle$$

  The scattering wave function $|q_{c+1}^{scatt}\rangle$ and the pseudo version of the scattering wave function are set equal to $|u^{scatt}\rangle$. The reason is that both must not include any contribution from the head function. Remember that they do not obey the equations of the corresponding energy derivative wave functions! Then we project out the core wave function to obtain the all-electron version of scattering wave function

$$
\begin{aligned}
|q_{c+1}^{scatt}\rangle &= |u^{scatt}\rangle \\
|\tilde{\phi}^{scatt}\rangle &= |u^{scatt}\rangle \\
|\phi^{scatt}\rangle &= |u^{scatt}\rangle - \sum_{i=1}^{c} |\phi_i\rangle\langle\phi_i|u^{scatt}\rangle
\end{aligned}
$$

- calculate pseudo density:
  - We determine the PAW bound states using the same boundary conditions as the all-electron calculation (typically a hard box with radius equal to the third grid point from the outside.)

$$\left[\frac{\vec{p}^2}{2m} + v - \epsilon_n\right]|\psi_n\rangle = 0$$

$$\left[\frac{\vec{p}^2}{2m} + \tilde{v} - \epsilon_n + \sum_{\alpha,\beta} |\tilde{p}_\alpha\Big(dH_{\alpha,\beta} - \epsilon_n dO_{\alpha,\beta}\Big)\langle\tilde{p}_\beta|\right]|\tilde{\psi}_n\rangle = 0$$

    The energies are determined independently. A deviation of the PAW bound energy from the original all-electron energy larger than 10^{-2} H, will cause an error message.

- Determine projections $\langle\tilde{p}_\alpha|\tilde{\psi}_n\rangle$.
- Normalize the all-electron and pseudo wave functions so that

$$\langle\tilde{\psi}_n|\tilde{\psi}_n\rangle + \sum_{\alpha,\beta}\langle\tilde{\psi}_n|\tilde{p}_\alpha\rangle dO_{\alpha,\beta}\langle\tilde{p}_\beta|\tilde{\psi}_n\rangle = 1$$

$$\langle\psi_n|\psi_n\rangle = 1$$

  The sign of the all-electron wave function is changed if it is inconsistent with the corresponding pseudo wave function.
- The densities are determined

$$n(\vec{r}) = \sum_n f_n\psi_n^*(\vec{r})\psi_n(\vec{r})$$

$$\tilde{n}(\vec{r}) = \sum_n f_n\tilde{\psi}_n^*(\vec{r})\tilde{\psi}_n(\vec{r})$$

- unscreening: The potential $\bar{v}(\vec{r})$ is constructed sich that

$$\tilde{v}(\vec{r}) = \bar{v}(\vec{r}) + \int d^3r' \, \frac{e^2\tilde{n}(\vec{r'}) + e^2Z(\vec{r'})}{4\pi\epsilon_0|\vec{r}-\vec{r'}|} + \mu_{xc}([\tilde{n}],\vec{r})$$

3.3 ATOMLIB$AESCF

This routine performs a selfconsistent all-electron calculation for a spherical, non-spin-polarized all-electron atom.

The boundary conditions are chosen such that there is a node at ROUT, which is currently set (outside the routine) to the third radial grid point from the end.

The operation of the subroutine is directed by a text variable "key".

- NONREL or REL: specified a relativistic or non-relativistic calculation.
- NONSO or SO: switches spin orbit coupling on or off. (the option SO is not implemented.)
- START: initializes occupations, angular momenta, starting potential, etc.

The orbitals are filled in the sequence

n	ℓ
1	0
2	0,1
3	0,1
4	0,2,1
5	0,2,1
6	0,3,2,1
7	0,3,2,1

for spin-orbit coupling each multiplet is divided into a 2ℓ states with antiparallel spin and orbit and $2\ell+2$ parallel states.

In the end of the self-consistent calculations the states are ordered according to increasing energues.

Dirac equation

The Dirac equation for the large component has the form

$$\left\{(1+D)\frac{\hat{p}^2}{2m}+V-\epsilon-\frac{\hbar^2}{2m_0}[\partial_r,D]_-\partial_r+\frac{[\partial_r,D]_-}{m_0|\vec{r}|}\vec{L}\vec{S}\right\}|\phi\rangle=0$$

where D is the measure for relativistic effects

$$D(r)=\frac{m_0}{M}-1=\frac{-1}{1+\frac{2m_0c^2}{\epsilon-V(\vec{r})}}$$

with M the relativistic mass. $D(\vec{r})$ is recalculated in each step for the corresponding energy. For non-relativistic calculations $D(r)$ is set to zero.

For a spherical potential we obtain the radial Dirac equation for the large component.

$$\left\{(1+D)\left[-\frac{1}{2r}\partial_r^2 r+\frac{\ell(\ell+1)}{2r^2}\right]-\frac{1}{2}D'\partial_r+\frac{X}{2r}D'+V-e\right\}R(r)=0$$

where $D'(r)=\partial_r D(r)$ and

$$X=\begin{cases}\ell & \text{for parallel spin and orbital angular momentum}\\ -\ell-1 & \text{for anti-parallel spin and orbital angular momentum}\\ 0 & \text{for a scalar relativistic equation}\end{cases}\tag{3.1}$$

Attention! At this point the small component is neglected both for the normalization and for the charge density.

Potential of the nucleus

The nucleus is considered as a homogeneously charged sphere. The volume of the nucleus is proportional to the number of nucleons. This allows to relate the radius directly to the mass of the nucleus.[5, 6]

$$r_{nuc}=\sqrt[3]{\frac{M}{u}}\cdot 1.2\cdot 10^{15}m=\sqrt[3]{\frac{M}{m_e}}\cdot 1.85635065215\cdot 10^{-6}a_0$$

where M is the mass of the nucleus and $u=\frac{1}{12}m(C^{12})$.

The potential of the nucleus is therefore

$$v_{nuc}(r)=\begin{cases}\frac{-Ze^2}{r_{nuc}}\left(\frac{3}{2}-\frac{1}{2}\frac{r^2}{r_{nuc}^2}\right) & \text{for} \quad r<r_{nuc}\\ \frac{-Ze^2}{r} & \text{for} \quad r>r_{nuc}\end{cases}$$

Potential: ATOMLIB$BOXVOFRHO

Calculates the output potential for a given chargedensity.

The integrations are performed only up to a selected radius RAD. In order to do the interpolation properly, the density must have a zero at the radius, and it must be specified for two grid points beyond RAD.

First we determine Hartree energy and potential:

Determine total charge

$$Q = \int d^3r\ \rho(\vec{r}) - Z$$

and then determine

$$v_H(\vec{r}) = \begin{cases} v_{nuc}(\vec{r}) + \int d^3r'\ \frac{e^2\rho(\vec{r'})}{4\pi|\vec{r}-\vec{r'}|} + \Delta_H & \text{for} \quad r < RAD \\ -\frac{Q}{|\vec{r}|} & \text{for} \quad r > RAD \end{cases}$$

$$\begin{aligned} E_H &= \frac{1}{2}\int d^3r\ \frac{e^2\rho(\vec{r})\rho(\vec{r'})}{4\pi|\vec{r}-\vec{r'}|} + \int d^3r\ \rho(\vec{r})v_{nuc}(\vec{r}) \\ &= \frac{1}{2}\int d^3r\ \rho(\vec{r})v_H(\vec{r}) + \frac{1}{2}\int d^3r\ \rho(\vec{r})v_{nuc}(\vec{r}) \end{aligned}$$

The variable Δ_H is determined such that v_{nuc} is continuous at RAD. The first expression for the Hartree energy is one that is easily recognized, while the second expression is the way it is actually calculated.

Now we determine the exchange-correlation energy and potential:

The routine that determines exchange-correlation and potential and energy takes the arguments: $\rho_t, \rho_s.(\vec{\nabla}\rho_t)^2, (\vec{\nabla}\rho_s)^2, (\vec{\nabla}\rho_t)(\vec{\nabla}\rho_s)$. Because the calculation does not include spin, only the arguments ρ_t and $(\vec{\nabla}\rho_t)^2$ will be required. Because the density is spherical we can furthermore use $(\vec{\nabla}\rho_t)^2 = (\partial_r\rho_t)^2$.

$$\begin{aligned} E_{xc} &= \int d^3r\ F(\rho, (\vec{\nabla}\rho)^2) \\ dE_{xc} &= \int d^3r\ \left[\frac{\partial F}{\partial\rho}d\rho + \frac{\partial F}{\partial(\vec{\nabla}\rho)^2)}(2\vec{\nabla}\rho)\vec{\nabla}d\rho\right] \\ &= \int_\Omega d^3r\ \left[\frac{\partial F}{\partial\rho}d\rho - \vec{\nabla}\left(\frac{\partial F}{\partial(\vec{\nabla}\rho)^2)}(2\vec{\nabla}\rho)\right)d\rho + \vec{\nabla}\left(\frac{\partial F}{\partial(\vec{\nabla}\rho)^2)}(2\vec{\nabla}\rho)d\rho\right)\right] \\ &= \int d^3r\ \theta_\Omega(\vec{r})\left[\frac{\partial F}{\partial\rho}d\rho - \vec{\nabla}\left(\frac{\partial F}{\partial(\vec{\nabla}\rho)^2)}(2\vec{\nabla}\rho)\right)d\rho\right] - \int d^3r\ \left(\vec{\nabla}\theta_\Omega(\vec{r})\right)\left(\frac{\partial F}{\partial(\vec{\nabla}\rho)^2)}(2\vec{\nabla}\rho)d\rho\right) \end{aligned}$$

Here $\theta_\Omega(\vec{r})$ is a step function which is equal to one within the integration volume Ω and zero outside. Its gradient is a δ function on the surface of the integration volume multiplies with an **inward-pointing** normal vector. The delta like contribution to the potential at the sphere surface is ignored. The simple reason is that the density vanishes at the surface, and it is hoped that F, and its derivative behave similarly. The more solid argument, which however is not very straightforward, is that the variation of the density at the sphere surface vanishes. This implies that the Lagrange parameter, the potential, is not needed at this point, and that any potential would not contribute to energy eigenvalues, for example.

The potential is determined as

$$\begin{aligned} v_{xc}(\vec{r}) &= \frac{\partial F}{\partial \rho} - \vec{\nabla}\left(\frac{\partial F}{\partial(\vec{\nabla}\rho)^2)} 2\vec{\nabla}\rho\right) \\ &= \frac{\partial F}{\partial \rho} - \vec{\nabla}\left(\frac{\partial F}{\partial(\vec{\nabla}\rho)^2)} 2\frac{\vec{r}}{|\vec{r}|}\partial_r\rho\right) \\ &= \frac{\partial F}{\partial \rho} - \left[\vec{\nabla}\frac{\vec{r}}{|\vec{r}|}\right]\left(\frac{\partial F}{\partial(\vec{\nabla}\rho)^2)} 2\partial_r\rho\right) - \frac{\vec{r}}{|\vec{r}|}\vec{\nabla}\left(\frac{\partial F}{\partial(\vec{\nabla}\rho)^2)} 2\partial_r\rho\right) \\ &= \frac{\partial F}{\partial \rho} - \left[\frac{2}{r}\right]\left(\frac{\partial F}{\partial(\vec{\nabla}\rho)^2)} 2\partial_r\rho\right) - \partial_r\left(\frac{\partial F}{\partial(\vec{\nabla}\rho)^2)} 2\partial_r\rho\right) \end{aligned}$$

The exchange correlation potential is set to zero if the density falls below a minimum of $10^{-6}\ a_0^{-3}$.

3.4 Setups_newpro

3.4.1 Input variables

The major input parameters are:

L	main angular-momentum quantum number
SO	spin-orbit allignment sgn($\vec{S}\vec{L}$) (SO$\in \{-1, 0, 1\}$)
ROUT	bound states are calculates in a box with radius ROUT
RC	cutoff for pseudization of partial waves
ENU	energy for Taylor expansion of partial waves

3.4.2 Flow chart

The flow of the subroutine is as follows:

1. nodeless core wave functions `UCORE`
2. coefficients `QN` for the expansion of node-reduced partial waves
3. energy dertivative partial wave of highest partial wave `QNDOT`
4. pseudo core wave functions `PSCORE`
5. pseudo partial waves `PSPHI` (without core tails)
6. all-electron partial waves `AEPHI` by core orthogonalization
7. bare projector functions `PRO`
8. bi-orthogonalization
9. matrix elements `DTKIN DOVER`

Pseudo core wave functions

We construct the function

$$\begin{aligned} f_1 &= r^\ell \\ f_2 &= r^{\ell+2} \\ f_3 &= r^{\ell+4} \end{aligned} \tag{3.2}$$

to the nodeless core wave function so that value and derivative agree at the pseudization radius.

Appendix A

Remarks

- The small contribution introduces nodes for the nodeless wave functions that lie near the nucleus which must not be counted. It is a consequence of treating the small component. This is taken care off by changing `schroedinger$phaseshift` so that nodes are counted starting with a minimum radius. Schade[4] gives the minimum radus of 0.07 a_0 for the core states and 0.09 a_0 for the valence states.
- Zora avoids the small component.?? Scalar relativistic calculations should treat the small component.
- Currently the pseudo partial waves do not contain a pseudo core contribution. The pseudo core contribution can introduce ghost states. On the other hand the pseudo core part lets the all-electron and pseudo partial waves to deviate at larger distances. Does this affect introduce an effect between core states and exponentially increasing partial waves?
- The Taylor and the Secant equation are closely related. The equations differ only by the value of the chosen energy which is ϵ_ν in one case and ϵ_{n+j} in the other. Can this be exploited?
- we need a criterion for the quality of the augmentation: The Taylor expansion of $|q_n(\epsilon)\rangle$ may have a radially dependent convergence radius $\epsilon_c(r)$. For a truncated Taylor expansion there is a radius where it is better to leave out a term than to include it. Similar problems occur for the secant construction usually employed in the PAW method.

  We could use something like

$$Q(\epsilon) \stackrel{\text{def}}{=} \min_{\vec{c}} \sum_n \left| \langle f_n | \left[\tilde{h} - \epsilon + \sum_\alpha |\tilde{p}_\alpha\rangle (dH_{\alpha,\beta} - \epsilon dO_{\alpha,\beta}) \langle \tilde{p}_\beta | \right] | q'_n(\vec{c},\epsilon)\rangle \right|^2 \qquad \text{(A.1)}$$

  where $|f_n\rangle$ is some orthonormal basisset and $q'_n(\vec{c},\epsilon)\rangle$ is some kind of expansion for the partial waves with coefficients $\vec{c}$.
- I need a section about the finite nuclear size
- The fock contribution is not yet included in the new version.
- for a semi-core state one should include a bound state for semi-core and for the valence state. The equations are very similar so that formulations can be integrated well.

Appendix B

Useful formulas

$$(\vec{\sigma}\vec{a})(\vec{\sigma}\vec{b}) = \vec{a}\vec{b} + i\vec{\sigma}(\vec{a}\times\vec{b}) \tag{B.1}$$

$$\vec{r}\vec{\sigma}\chi_{\kappa,j_z} = -|\vec{r}|\chi_{-\kappa,j_z} \tag{B.2}$$

$$\vec{S}\vec{p}R(|\vec{r}|)\chi_{\kappa,j_z} = \frac{i\hbar^2}{2}\Big[\partial_r + \frac{\kappa+1}{|\vec{r}|}\Big]R(|\vec{r}|)\chi_{-\kappa,j_z} \tag{B.3}$$

$$1 + D = \frac{1}{1+\frac{\epsilon-v}{2m_0c^2}} \tag{B.4}$$

$$\kappa(\ell, so) = -1 + so\cdot\Big(\ell + \frac{so-1}{2}\Big) = \begin{cases} -\ell-1 & \text{for } \vec{L}\vec{S} \geq 0 \text{ .i.e. } so = 1 \\ \ell & \text{for } \vec{L}\vec{S} < 0 \text{ .i.e. } so = -1 \\ -1 & \text{for } \vec{L}\vec{S} = 0 \text{ .i.e. } so = 0 \end{cases} \tag{B.5}$$

Appendix C

Taylor expansion of node-reduced partial waves

Here we derive the coefficients $c_{m,j}$ used to determine the Taylor coeffcieients Eq. **??** of the all-electron partial waves from the nodeless core wave functions and the Taylor expansion coefficients Eq. 1.16 of the node-reduced wave functions.

$$\begin{aligned}
|\phi_n^{(j)}(\epsilon_\nu)\rangle &\overset{\text{Eq. ??}}{=} \frac{(-1)^j}{j!}\,\partial_\epsilon^j\big|_{\epsilon_\nu}\left[|\phi_n(\epsilon)\rangle\frac{1}{\prod_{k=1}^{n-1}(\epsilon_j-\epsilon)}\right]\\
&\overset{\text{Eq. 1.10}}{=} \frac{(-1)^j}{j!}\,\partial_\epsilon^j\big|_{\epsilon_\nu}\left[|q_n(\epsilon)\rangle+\sum_{m=1}^{n-1}|u_m\rangle\prod_{j=m}^{n-1}\frac{1}{\epsilon_j-\epsilon}\right]\\
&\overset{\text{Eq. 1.16}}{=} |q_n^{(j)}(\epsilon_\nu)\rangle+\sum_{m=1}^{n-1}|u_m\rangle\underbrace{\left(\frac{(-1)^j}{j!}\,\partial_\epsilon^j\big|_{\epsilon_\nu}\left[\prod_{j=m}^{n-1}\frac{1}{\epsilon_j-\epsilon}\right]\right)}_{c_{m,j}}
\end{aligned}\tag{C.1}$$

It is our goal to work out the coeffcients $c_{m,j}$. To explore the structure of the expressions let us evaluate the first two derivatives of the product terms

$$\begin{aligned}
\underbrace{\partial_\epsilon^0\big|_{\epsilon_\nu}\left[\prod_{j=m}^{n-1}\frac{1}{\epsilon_j-\epsilon}\right]}_{b_{m,0}} &= \underbrace{\left[\prod_{j=m}^{n-1}\frac{1}{\epsilon_j-\epsilon_\nu}\right]}_{b_{m,0}}\\
\underbrace{\partial_\epsilon^1\big|_{\epsilon_\nu}\left[\prod_{j=m}^{n-1}\frac{1}{\epsilon_j-\epsilon}\right]}_{b_{m,1}} &= \underbrace{\left[\prod_{j=m}^{n-1}\frac{1}{\epsilon_j-\epsilon_\nu}\right]}_{b_{m,0}}\underbrace{\left[\sum_{k=m}^{n-1}\frac{1}{\epsilon_j-\epsilon_\nu}\right]}_{a_{m,0}}
\end{aligned}\tag{C.2}$$

Let us now introduce the new symbols

$$b_{m,j} \stackrel{\text{def}}{=} \partial_\epsilon^j\big|_{\epsilon_\nu}\left[\prod_{j=m}^{n-1}\frac{1}{\epsilon_j-\epsilon}\right]$$
$$a_{m,j} \stackrel{\text{def}}{=} \partial_\epsilon^j\big|_{\epsilon_\nu}\left[\sum_{k=m}^{n-1}\frac{1}{\epsilon_j-\epsilon}\right] \tag{C.3}$$

Thus we obtain

$$\begin{aligned}
b_{m,1} &= b_{m,0}a_{m,0}\\
b_{m,2} &= b_{m,1}a_{m,0} + b_{m,0}a_{m,1}\\
b_{m,2} &= b_{m,2}a_{m,0} + 2b_{m,1}a_{m,1} + b_{m,0}a_{m,2}\\
b_{m,j} &= \sum_{k=0}^{j-1}\binom{j-1}{k}b_{m,j-k-1}a_{m,k}\\
\underbrace{\frac{(-1)^j}{j!}b_{m,j}}_{c_{m,j}} &= \sum_{k=0}^{j-1}\frac{(-1)^j}{j!}\underbrace{\frac{j-1)!}{(j-k-1)!k!}}_{\binom{j-1}{k}}b_{m,j-k-1}a_{m,k}\\
&= \sum_{k=0}^{j-1}\frac{+1}{j}\underbrace{\left[\frac{(-1)^{j-k-1}}{(j-k-1)!}b_{m,j-k-1}\right]}_{c_{m,j-k-1}}\left[-\frac{(-1)^k}{k!}a_{m,k}\right]
\end{aligned} \tag{C.4}$$

The coefficients $a_{m,k}$ are obtained as follows

$$a_{m,j} = \partial_\epsilon^j\big|_{\epsilon_\nu}\left[\sum_{k=m}^{n-1}\frac{1}{\epsilon_j-\epsilon}\right] = \left[\sum_{k=m}^{n-1}\frac{j!}{(\epsilon_j-\epsilon_\nu)^{j+1}}\right] \tag{C.5}$$

so that

$$-\frac{(-1)^j}{j!}a_{m,j} = +\sum_{k=m}^{n-1}\frac{1}{(\epsilon_\nu-\epsilon_j)^{j+1}} \tag{C.6}$$

Thus we obtain the following recursive set of equations

$$c_{m,0} = \prod_{j=m}^{n-1}\frac{1}{\epsilon_j-\epsilon} \tag{C.7}$$

$$c_{m,j} = \frac{1}{j}\sum_{k=0}^{j-1}c_{m,j-k-1}d_{m,k} \qquad \text{for } j=1,\ldots,\infty$$

$$d_{m,j} = \left[\sum_{k=m}^{n-1}\frac{1}{(\epsilon_j-\epsilon_\nu)^{j+1}}\right] \qquad \text{for } j=0,\ldots,\infty \tag{C.8}$$

with which we can evaluate the true wave functions in the form

$$|\phi_n^{(j)}(\epsilon_\nu)\rangle = |q_n^{(j)}(\epsilon_\nu)\rangle + \sum_{m=1}^{n-1}|u_m\rangle c_{j,m} \tag{C.9}$$

Appendix D

Derivation of inhomogeneity for the radial Dirac equation

Here I make the derivation of the inhomogenity of the radial Dirac equation very explicit so that one can follow all the signs. This is because I changed the sign convention of the nodeless construction, which may cause a mixup with earlier results.

$$\begin{aligned}
&-|u_{n-1}\rangle - (\vec{S}\vec{p})\frac{1+D}{\hbar m_0 c}|v_{n-1}\rangle \\
&-g^{n-1}_{\kappa,j_z} - \frac{i\hbar^2}{2}\Big(\partial_r + \frac{1-\kappa}{|\vec{r}|}\Big)\frac{1+D}{\hbar m_0 c}\Big(if^{n-1}_{-\kappa,j_z}\Big) \\
&\Big(-g^{n-1}_{\kappa,j_z}\Big) - \frac{\hbar}{c}\Big(\partial_r + \frac{1-\kappa}{|\vec{r}|}\Big)\frac{1+D}{2m_0}\Big(-f^{n-1}_{-\kappa,j_z}\Big)
\end{aligned} \tag{D.1}$$

$$\begin{aligned}
|v_n\rangle &= \frac{1+D}{2m}\Big[\frac{2}{\hbar c}(\vec{S}\vec{p})|u_n\rangle + \frac{1}{c}v_n\rangle \\
if^n_{-\kappa,j_z} &= \frac{1+D}{2m}\Big[\frac{2}{\hbar c}\frac{i\hbar^2}{2}\Big[\partial_r + \frac{1+\kappa|}{|\vec{r}|}\Big]g^{(n)}_{\kappa,j_z} + \frac{1}{c^2}\Big(if^{(n)}_{-\kappa,j_z}\Big)\Big] \\
f^n_{-\kappa,j_z} &= \frac{1+D}{2m}\Big[\frac{\hbar}{c}\Big[\partial_r + \frac{1+\kappa|}{|\vec{r}|}\Big]g^{(n)}_{\kappa,j_z} + \frac{1}{c^2}\Big(f^{(n)}_{-\kappa,j_z}\Big)\Big]
\end{aligned} \tag{D.2}$$

Appendix E

Parameters for the Setup construction

E.0.3 Parameters for the HBS-type construction

```
!SETUP ID='CA_HBS' EL='CA'  ZV=2
   RBOX/RCOV=2.0  RCSM/RCOV=0.25
   TYPE='HBS'
   RCL/RCOV=0.75 0.75 0.75 LAMBDA=6. 6. 6.
   !GRID DMIN=5.E-6 DMAX=0.1 RMAX=7.2 !END
   !POT   POW=3. VAL0=-1.2 RC/RCOV=0.67 !END
   !CORE  POW=2. VAL0= 0.1 RC/RCOV=0.67 !END
!END

!SETUP ID='CA_SC_HBS' EL='CA'  ZV=10.
   RBOX/RCOV=2. RCSM/RCOV=0.25
   TYPE='HBS'
   RCL/RCOV=0.5 0.5 0.5 0.5  LAMBDA=6. 6. 6. 6.
   !GRID DMIN=5.E-6 DMAX=0.1 RMAX=7. !END
   !POT   POW=3. VAL0=-2.2 RC/RCOV=0.5 !END
   !CORE  POW=2. VAL0= 0.1 RC/RCOV=0.5 !END
!END
```

For valence-only setups use the following set for the partial waves $r_c = 0.75 r_{cov}$, $\lambda = 6$.

For semi-core setups use the following set ofr the partial waves $r_c = 0.55 r_{cov}$, $\lambda = 6$.

The decay parameter for the compensation charge density should be set to $0.25 r_{cov}$.

It is beneficial if the pseudopotential follows the all-electron potential inward further than the covalent radius.

Usually, we do not specify the parameter VAL0 for the potential. This however causes problems for transition metals, where we obtain ghost states.

Index

Bibliography

[1] P. E. Blöchl and C. Först. Node-less atomic wave functions, pauli repulsion and systematic projector augmentation. Arxiv, 1210.5937, 2012. URL http://arxiv.org/abs/1210.5937.

[2] Erik van Lenthe. The Zora Equation. PhD thesis, Vrije Universiteit Amsterdam, 1996.

[3] Leslie L. Foldy and Siegfried A. Wouthuysen. On the dirac theory of spin 1/2 particles and its non-relativistic limit. Phys. Rev., 78:29, 1950.

[4] Robert Schade. Relativistic effects in the paw method beyond the scalar approximation. Master's thesis, Göttingen University, 2012.

[5] L. N. Cooper and E. M. Henley. Mu-mesonic atoms and the electromagnetic radius of the nucleus. Phys. Rev., 92:801–811, Nov 1953. doi: 10.1103/PhysRev.92.801. URL http://link.aps.org/doi/10.1103/PhysRev.92.801.

[6] Robert Hofstadter. Electron scattering and nuclear structure. Rev. Mod. Phys., 28:214–254, Jul 1956. doi: 10.1103/RevModPhys.28.214. URL http://link.aps.org/doi/10.1103/RevModPhys.28.214.

[7] J. Paier, R. Hirschl, M. Marsman, and G. Kresse. The perdew-burke-ernzerhof exchange-correlation functional applied to the g2-1 test set using a plane-wave basis set. J. Chem. Phys., 122:234102, 2005.